

Policy Selection and Schedules for Exclusive Bus Lane and High Occupancy Vehicle Lane in a Bi-modal Transportation Corridor

Jiaqing Lu

Department of Civil and Environmental Engineering,

Florida State University

2525 Pottsdamer St, Tallahassee, FL 32310

jl23br@fsu.edu

Qian-wen Guo, Ph.D. (corresponding author)

Department of Civil and Environmental Engineering,

Florida State University

2525 Pottsdamer St, Tallahassee, FL 32310

qguo@fsu.edu

Paul Schonfeld, Ph.D.

Department of Civil and Environmental Engineering,

University of Maryland, College Park

1173 Glenn Martin Hall, College Park, MD 20742 US

pschon@umd.edu

Abstract

Efficient management of transportation corridors is critical for sustaining urban mobility, directly influencing transportation efficiency. Two prominent strategies for enhancing public transit services and alleviating congestion, Exclusive Bus Lane (EBL) and High Occupancy Vehicle Lane (HOVL), are gaining increasing attention. EBLs prioritize bus transit by providing dedicated lanes for faster travel times, while HOVLs encourage carpooling by reserving lanes for high-occupancy vehicles. However, static implementations of these policies may underutilize road resources and disrupt general-purpose lanes. Dynamic control of these policies, based on real-time demand, can potentially maximize road efficiency and minimize negative impacts. This study develops cost functions for Mixed Traffic Policy (MTP), Exclusive Bus Lane Policy (EBLP), and High Occupancy Vehicle Lane Policy (HOVLP), incorporating optimized bus frequency and demand split under equilibrium condition. Switching thresholds for policy selection are derived to identify optimal periods for implementing each policy based on dynamic demand simulated using an Ornstein-Uhlenbeck (O-U) process. Results reveal significant reductions in total system costs with the proposed dynamic policy integration. Compared to static implementations, the combined policy achieves cost reductions of 12.0%, 5.3% and 42.5% relative to MTP-only, EBLP-only, and HOVLP-only scenarios, respectively. Additionally, in two real case studies of existing EBL and HOVL operations, the proposed dynamic policy reduces total costs by 32.2% and 27.9%, respectively. The findings provide valuable insights for policymakers and transit planners, offering a robust framework for dynamically scheduling and integrating EBL and HOVL policies to optimize urban corridor efficiency and reduce overall system costs.

Keywords: Policy selection and schedules; Exclusive bus lane; High occupancy vehicle lane; Transportation corridor; Modal competition

1. Introduction

A transportation corridor typically encompasses multiple transportation modes, with automobiles and bus serving as primary options for long distance travel (Hossain and McDonald, 1998; Li et al., 2012). The complex interactions of different vehicles within general-purpose lanes significantly influence the efficiency, sustainability and overall performance of urban transportation corridors (Yao et al., 2012 and 2015). However, rising population density and urbanization have intensified traffic congestion, making inefficient traffic management a pressing challenge (Wang et al., 2024). To address this issue, city administrators often implement various traffic management policies to optimize road infrastructure usage and promote public transit (Li et al., 2020).

One notable policy employed to enhance the efficiency of public transit is the Exclusive Bus Lane (EBL), which designated a dedicated lane for buses (Basso et al., 2011). The EBL concept emerged in the U.S. during the 1960s and 1970s as a response to the growing need for improved public transportation and reduce congestion. For example, in Seattle, one lane of 3rd Avenue, the city's busiest bus corridor, is reserved for buses and emergency vehicles during peak hours, significantly reducing delays and improving service reliability (Seattle Department of Transportation). Dedicated bus lanes allow buses to operate with lower equivalent traffic volume than the general-purpose lanes, enabling faster travel and more reliable schedules (Navarrete-Hernandez and Zegras, 2023). EBLs offer numerous benefits to public transit systems, such as improving passenger satisfaction, decreasing accidents and reducing emissions (Goh et al., 2014).

Empirical evidence supports the effectiveness of EBLs. Russo et al. (2022) reported that bus travel time and passenger waiting time decreased by about 18% and 12% respectively after implementing an EBL. Similarly, simulation studies by Kim et al. (2019) showed that corridor energy consumption could decrease by 18.5%, and emissions could drop by 19.3-31.4% for various pollutants along a Seoul corridor. Additionally, EBLs improves the service quality, attracting more passengers to public transit systems (Chow et al., 2011; Othman and Abdulhai, 2023).

Despite these advantages, challenges remain. EBL implementation often reallocating road space,

accommodating diverse road users, and redesigning intersections for traffic signal and lane markings (Wu et al., 2017). Critics argue that EBLs can intensify congestion in general-purpose lanes, potentially worsening the unequal distribution of road resources (Kittelson and Associates, 2003). In some cases, such as Flagler Street in Miami and Richmond Avenue in Houston, EBLs were removed due to their failure to improve bus speeds and the worsening of traffic congestion. Excessive implementation of EBLs can also negatively impact a transportation system's operational efficiency, as demonstrated by optimization models for multi-modal transportation networks (Yao et al., 2012). Consequently, decisions on whether and when to introduce an EBL remain open questions which warrant further investigation.

High occupancy vehicle lanes (HOVLS) represent another prominent policy aimed at reducing single-occupancy vehicle usage by encouraging carpooling. Since the establishment of the first HOV lane on the Shirley Highway in Northern Virginia in 1969, this policy have been widely implemented in cities such as Seattle (I-5), Houston (I-45), Miami (I-95), and Los Angeles (I-110) (Yang and Huang, 1999). HOVLS, providing a dedicated lane for High-Occupancy Vehicles, not only reduces the number of vehicles due to increased carpooling but also improves travel time predictability and reliability for carpoolers (Cohen et al., 2022). HOVLS have received significant attention for their environmental benefits (Boriboonsomsin and Barth, 2008; Javid et al., 2017; Sharifi et al., 2022; Fontes et al., 2014), their influence on carpooling behavior (Zhong et al., 2020; Boysen et al., 2021; Cohsen et al., 2022), and their planning considerations (Dahlgren et al., 1998; Stamos et al., 2012; Wiseman, 2019; Li et al., 2020). However, implementing HOVLS presents several challenges, such as the need for strict enforcement of occupancy criteria, which may require additional enforcement resources (Brownstone et al., 2003). Moreover, the effectiveness of HOV lanes may be limited in areas with dispersed populations, raising questions about the suitability of this policy in certain regions (Chu et al., 2012).

To maximize policy effectiveness under constrained road resources, the policy selection problem involves determining whether a transportation corridor should designate a lane as an EBL or a HOVL. The trade-off balances the increased congestion for auto mobiles caused by reduced road capacity with the benefits of improved bus and HOV operations. Some studies have explored the circumstances for EBL

or HOVL implementation and their optimal allocation (Wang and Li, 2014; Wang et al., 2019; Lu et al., 2023). For EBL, guidelines suggest implementation when bus volumes reach 20-30 buses per hour (Teer et al. 1994), 30-40 buses per hour (The Transit Cooperative Research Program (TCRP), 2013), or 70 buses per hour (Levinson et al., 1991). However, using only bus demand as the criterion for implementing an EBL would overlook its effects on auto users. Yao et al. (2015) assessed the EBL selection in a bi-modal network considering risk-adverse travelers, later expanding to a tri-modal network incorporating carpooling (Yao et al., 2018). For the HOVLs, Yang (1998) proposed a cost-effectiveness measure to assess feasibility, while Zhou et al. (2020) evaluated per capita delay impacts. However, most studies have focused on network-wide or intersection-based applications with static setting.

Dynamic or intermittent policies offer a practical approach for EBL or HOVL scheduling. Proper scheduling based on demand thresholds is crucial for maximizing policy benefits. For instance, Zhao et al. (2018) found intermittent EBLs reduced average delay by over 10% at intersections, while Szarata et al. (2021) demonstrated that dynamic bus lanes yielded better bus service benefits with minimal private car delays compared to permanent EBLs. Othman et al. (2023) confirmed the effectiveness of dynamic EBLs across various demand levels, and Zhou et al. (2020) proposed dynamic HOVL controls that reduced total vehicle miles traveled (VMT) by 4.93% and per capita travel time by 4.27%.

Successful implementations of intermittent EBLs in cities such Lisbon, Melbourne, and Eugene have improved transit speeds by 8-20% (Viegas & Lu, 2004; Currie & Lai, 2008). Signal control enables real-time policy switching, enabling its operational use (Levin & Khani, 2018). However, prior studies focus on dynamic policy optimization without addressing specific road schedules or considering bus operators' interests. Moreover, most dynamic models neglect the time-variant nature of corridor demand under uncertainties. For instance, existing literature often prescribes EBLs based on general peak traffic patterns rather than quantitatively identifying optimal operation periods (Chiabaut & Barcet, 2019; Othman et al., 2023).

Our research addresses these gaps by quantitatively determining the optimal operation times for Exclusive Bus Lanes (EBLs) to improve lane management strategies. Effective scheduling of EBLs can

enhance performance across multiple modes without disproportionately disadvantaging any single mode (Khoo et al., 2014). Previous models, such as those by Ho (2013) and Khoo & Ong (2015), integrated bi-level optimization with traffic simulations to focus on network-wide travel time minimization. However, our model expands upon this by considering both travel time and intersection delays, offering a more comprehensive assessment of policy impacts. By incorporating diverse cost factors and realistic demand fluctuations, our approach aims to optimize the selection and implementation timing of policies across varying demand densities.

Demand density significantly impacts the costs of transportation systems for both auto and bus modes. The ratio between bus and auto traffic fluctuates throughout the day and in response to various conditions, reflecting the dynamic nature of transportation demand. For example, during peak hours, bus demand may increase sharply, while at other times, private auto usage dominates. These fluctuations are influenced by factors such as time of day, weather, and special events, making demand patterns inherently unpredictable. The Ornstein-Uhlenbeck (OU) process, which captures both short-term randomness and long-term trends, offers an effective framework for modeling these variations in the bus-to-auto ratio (Coscia et al., 2018). This capability aids in optimizing transportation policies, such as Exclusive Bus Lanes and mixed-traffic management, by accurately simulating demand fluctuations and supporting more informed decision-making. To capture this variability, we simulate demand over time using the OU process, which models natural oscillations and trends (Berling & Martínez-de-Albéniz, 2011; Guo et al., 2017).

To model the policy selection and scheduling problem, three policies were formulated for implementation in the transportation corridor, as depicted in Figure 1. In a mixed traffic policy (MTP), autos and buses share road lanes in the corridor, leading to interactions among them. In the exclusive bus lane policy (EBLP), a dedicated lane in the corridor is reserved exclusively for buses. This separation ensures that buses and autos do not affect each other, as neither can encroach upon the other's designated lane. In the high-occupancy vehicle lane policy (HOVLP), a specific lane is designated as a high-occupancy vehicle lane, allowing both high occupancy autos and buses exclusive use of this lane. By specifying the three policies, the schedule can be optimized by determining the ideal switching thresholds

between them.

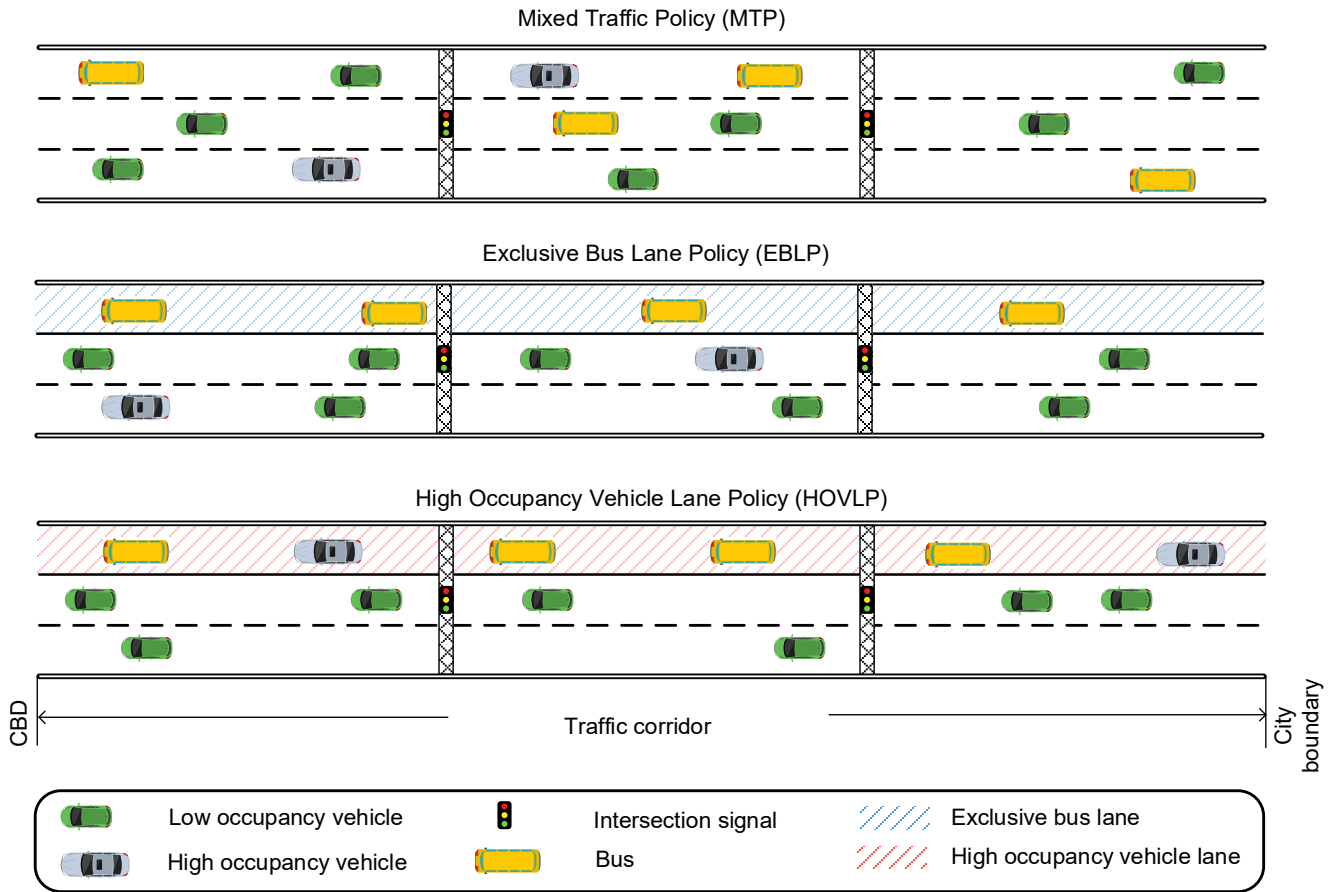


Figure 1. Transportation corridor under different traffic policies

The main contributions of this study are as follows:

- 1) In a transportation corridor, mode choice equilibrium is employed to allocate the demand density so that individual travelers chose the least costly travel mode between bus and auto;
- 2) Thresholds for different policy are jointly determined with optimized bus frequencies to minimize the total system cost;
- 3) A sensitivity analysis of road capacity is conducted to evaluate its impact on the total system cost;
- 4) The demand density is simulated with an O-U process, and the feasible policy scheduling periods for different policies are identified;
- 5) Two case studies and an experiment are examined to verify the benefits of our proposed policy scheduling model for EBL and HOVL in a bi-modal transportation corridor.

The rest of this paper is organized as follows. Section 2 describes the travel demand and establishes cost functions of three policies representing different policies. In Section 3, the policy selection model and scheduling model are introduced for optimizing the switching timing between different policies and find the optimal operation duration for these policies based on simulated demand density. The goal is to minimize total system costs by dynamically selecting policies in response to changing traffic conditions. In Section 4, the total cost of different policies and their switching thresholds are identified jointly with optimized bus frequency. The effectiveness of dynamic policy selection and scheduling in response to changing demand density is demonstrated through policy selection and schedule model analysis. Through experiment and two real-world case studies, the implementation of our proposed policy scheduling showcases significant cost savings. Finally, conclusions and future research directions are discussed in Section 5.

2. Problem formulation

To clearly define our model, all notations are listed in Table 1.

Table 1. Notation list

Parameters	Definitions
A	Distance between CBD and city boundary
C	Lane capacity
C_O^f	Fixed cost of bus operation
C_O^v	Variable cost of bus operation
C_e^f	Fixed cost of EBL signal implementation
C_e^v	Variable cost of EBL signal implementation
C_h^f	Fixed cost of HOVL signal implementation
C_h^v	Variable cost of HOVL signal implementation
C_{signal}	Cycle length in the intersection
C_p^a	Total travel cost of auto users under different policies
C_p^b	Total cost of the passengers' trips under different policies
C_p^O	Bus operating cost C_p^O under different policies
C_p^S	EBL/HOVL signal implementation cost
d_{ma}^i	Intersection delay per auto at intersection i under MTP
d_{mb}^i	Intersection delay per bus at intersection i under MTP
d_{eb}^i	Intersection delay per bus at intersection i under EBLP
d_{hb}^i	Intersection delay per bus at intersection i under HOVL
d_{ea}^i	Intersection delay per auto at intersection i under EBLP
d_{hla}^i	Intersection delay per low occupancy auto at intersection i

d_{hha}^i	Intersection delay per high occupancy auto at intersection i under MTP
D_p^b	Total intersection delay of buses in the transportation corridor under different policies
D_p^a	Total intersection delay of autos in the transportation corridor under different policies
F_p	Bus service frequency under different policies
K	Factor converting a bus into a number of autos with equivalent effect on traffic
f_b	Flat fare paid per bus trip
l_i	Location of intersection i
n_{lane}	The number of lanes in transportation corridor
n_{inter}	The number of intersections in transportation corridor
n_Γ	The number of schedule periods in the set Γ
O_a	Average auto occupancy
O_{la}	Occupancy rate of low occupancy auto
O_{ha}	Occupancy rate of high occupancy auto
O_b	Bus capacity
q_0	Demand density in the CBD
t^{entry}	Starting point from one policy to another
t^{exit}	Exiting point from one policy to another
t_l	Duration of the analysis setting method
t_0^a	Free-flow auto travel time per unit of distance
t_0^b	Free-flow bus travel time per unit of distance
W	Cumulative cost in the schedules period
Z	Total cost saving
α^a	Corrected parameter of BPR function
α^b	Corrected parameter of BPR function
β^a	Corrected parameter of BPR function
β^b	Corrected parameter of BPR function
ε_t^b	Value of in-vehicle time of bus travelers
ε_t^a	Value of in-vehicle time of auto users
δ_f^a	Fixed cost of auto usage
δ_v^a	Variable cost of auto usage
l_1	Positive parameters in discomfort function
l_2	Positive parameters in discomfort function
μ	The fraction of low-occupancy autos over total autos
γ_1	A positively calibrated parameter that depends on the bus headway.
γ_2	A positive parameter that is used to calibrate the distribution of passenger arrival times
γ_3	A positive parameter that is used to calibrate the distribution of passenger arrival times
q_l	Fraction of low-occupancy auto travelers over total number of auto travelers
q_h	Fraction of high-occupancy auto travelers over total number of auto travelers
λ	Green signal ratio of the lane
κ	Incremental delay factor accounting for pre-timed signal controller settings
φ	Adjustment factor for upstream filtering
v	Mean reversion parameter
\bar{w}	Long-term ratio of the O-U process
σ	Volatility of the O-U process
Γ	Feasible lane policy schedule set

2.1 Assumptions

A1 The corridor connecting the city's Central Business District (CBD) and suburban area is modeled as linear. This linear representation is chosen to simplify the analysis and enable the formulation of a macroscopic cost function. Such an approach has been widely adopted in previous studies to facilitate analytical modeling and computational tractability (e.g., Wang et al., 2004; Liu et al., 2009; Sun et al., 2017; Guo et al., 2021; Guo et al., 2023; Yu et al., 2023).

A2 Our research focuses on a many-to-one travel demand pattern, where multiple travelers are headed toward a CBD (Zhang et al., 2005). The travelers demand distribution along the corridor is specified as a linear function (Li et al., 2015; Sun et al., 2017; Guo et al., 2018). The demand density at distance x from CBD is represented as $q(x) = q_0 - \frac{q_0}{A}x$, $\forall x \in (0, A]$, where q_0 is the demand density in the CBD and the demand density at the city boundary is zero. Based on the mode choice equilibrium model, commuters select the most cost-effective mode of transportation along the corridor for their journeys to the CBD, regardless of their starting location (Ho et al. 2005 and Xu et al. 2014).

A3 The effect of overcrowding in buses can be represented through a discomfort cost function, as discussed in previous research by Huang (2002), Li et al. (2009), and Guo et al. (2021).

A4 It is assumed that all intersections are evenly spaced along the corridor, as illustrated in Figure 2. Therefore, the location of intersection i can be represented by the expression $l_i = \frac{A}{n_{inter}+1} * i$, where A denotes the total length of the corridor and n_{inter} represents the total number of intersections.

2.2 Travel demand

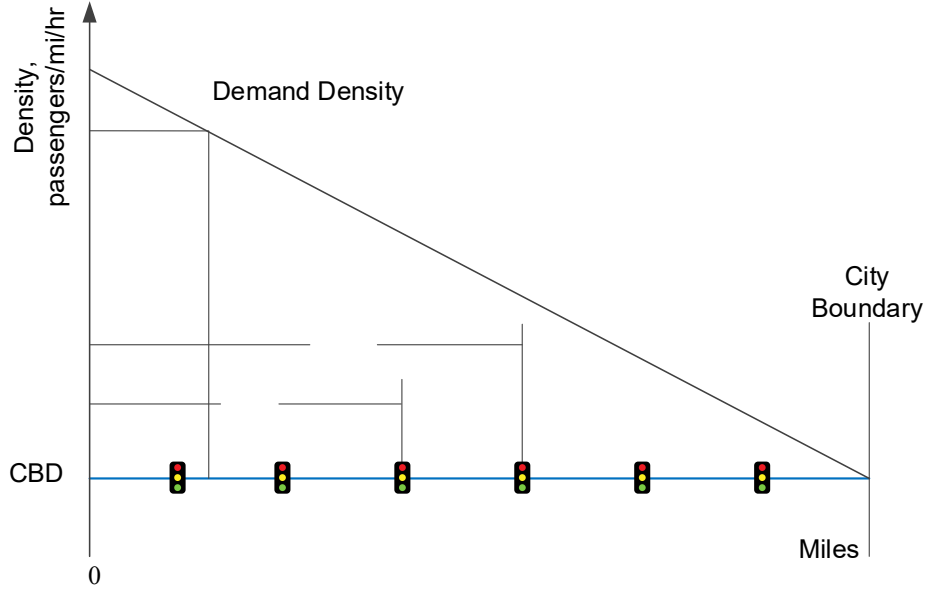


Figure 2. Illustration of the demand density function

As shown in Figure 2, the density of travel demand at location x is:

$$q(x) = q_0 - \frac{q_0}{A}x, \forall x \in (0, A], \quad (1)$$

where q_0 is the demand density in the CBD, A is the distance between CBD and city boundary, and the demand density at the city boundary is zero.

In a transportation corridor, two alternative modes are considered, auto and bus, sharing the same road lanes, as expressed in Eq. (2). It is assumed that during the morning peak hours, all commuters choose the less costly mode when traveling along the corridor to CBD. When everyone selects the least costly mode, the congested bimodal corridor reaches a user equilibrium state. In that state, the individual generalized travel cost by a mode at any location should be the minimum among the costs by the two modes if the mode is used by commuters at any location. Therefore, the equilibrium mode choice is used to split the demand in the bimodal corridor represented by Eq. (2). Appendix B provides the formulation and proof of this deterministic continuum equilibrium mode choice.

$$q(x) = q_a^*(x) + q_b^*(x) = R^*q(x) + (1 - R^*)q(x), \forall x \in (0, A]. \quad (2)$$

where $q_a^*(x)$ and $q_b^*(x)$ is the auto and bus demand at location x under equilibrium condition, R^*

represents the ratio of auto demand to total demand, and it is determined under equilibrium conditions, as outlined in Appendix B.

The traveler demand of bus/auto at location x is the cumulative demand density from city boundary to location x , which is expressed as:

$$Q_j(x) = \int_x^A q_j(w) dw, \forall x \in (0, A], \forall j = a, b, \quad (3)$$

where $j = b$ represents transit vehicle, and $j = a$ represents auto traffic.

Let $v(x)$ denote the total traffic volume including autos and buses at location $x \in (0, A]$:

$$v(x) = \frac{Q_a(x)}{O_a} + KF, \forall x \in (0, A], \quad (4)$$

where K is the physical equivalent factor to convert the traffic effect of a bus into that of a few autos, and F is the bus service frequency along the transportation corridor. O_a is average occupancy per auto, which can be obtained by Eq. (C6) in Appendix C.

2.3 System cost minimization

When the transportation corridor is operating under the mixed traffic policy where $x \in (0, A]$, the travel time per unit of distance at location x is obtained with the Bureau of Public Roads (BPR) function (Li et al., 2015), which can be expressed as:

$$t_m^j(x) = t_0^j \left(1 + \alpha^j \left(\frac{v(x)}{n_{lane} * C} \right)^{\beta^j} \right), \forall x \in (0, A], \forall j = a, b, \quad (5)$$

where t_0^j is the free flow auto/bus travel time per unit of distance, C is the lane capacity, n_{lane} represents the number of lanes in the corridor, α^j and β^j are the parameters under mixed traffic operation.

The travel time by bus/autos from location x to CBD $T_m(x)$ is:

$$T_m^j(x) = \int_0^x t_m^j(w) dw, \forall x \in (0, A], \forall j = a, b. \quad (6)$$

When the corridor is operating under EBLP, the auto and bus travel times per unit of distance are different, depending on the distance x to CBD. In contrast, the bus travel time per unit of distance is uniformly distributed along the corridor after the bus operating frequency F is determined. This can be expressed as:

$$t_e^a(x) = t_0^a \left(1 + \alpha^a \left(\frac{Q_a(x)}{O_a(n_{lane}-1)c} \right)^{\beta^a} \right), \quad \forall x \in (0, A]. \quad (7)$$

$$t_e^b(F) = t_0^b \left(1 + \alpha^b \left(\frac{KF}{c} \right)^{\beta^b} \right), \quad (8)$$

The travel time by bus from location x to CBD $T_e^b(x)$ under EBLP is:

$$T_e^b(x) = \int_0^x t_e^b(F) dw, \quad \forall x \in (0, A], \quad (9)$$

where $t_e^b(F)$ is the bus travel time per unit of distance in the corridor, which is determined by bus operating frequency F .

The travel time by auto from location x to CBD $T_e^a(x)$ under EBLP is:

$$T_e^a(x) = \int_0^x t_e^a(w) dw, \quad \forall x \in (0, A], \quad (10)$$

When the corridor operates under HOVLP, both the high-occupancy vehicles and buses share the high occupancy lane, resulting in the same travel time per unit of distance. The occupancy of low occupancy autos is O_{la} and the occupancy of high occupancy is O_{ha} . The fractions of low-occupancy auto travelers ρ_l and high-occupancy auto travelers ρ_h , relative to the total number of auto travelers can be determined based on the provided parameters, as explained in Appendix C. The travel time per unit distance for low-occupancy autos is expressed in Eq. (11). Buses and high-occupancy autos share the HOVL, resulting in identical travel times per unit distance, as specified in Eq. (12). Eq. (12).

$$t_h^{la}(x) = t_0^a \left(1 + \alpha^a \left(\frac{\rho_l Q_a(x)/O_{la}}{(n_{lane}-1)c} \right)^{\beta^a} \right), \quad \forall x \in (0, A]. \quad (11)$$

$$t_h^{ha}(x) = t_h^b(x) = t_0^j \left(1 + \alpha^j \left(\frac{\rho_h Q_a(x)/O_{ha} + KF}{c} \right)^{\beta^b} \right), \quad \forall x \in (0, A], \quad \forall j = a, b. \quad (12)$$

where la and ha in Eq. (11) and (12) represent low-occupancy auto and high-occupancy auto, μ is the fraction of low-occupancy autos over total autos.

The travel time by bus and high-occupancy vehicle from location x to CBD $T_h^j(x)$ under HOVLP is:

$$T_h^b(x) = \int_0^x t_h^b(w) dw, \quad \forall x \in (0, A], \quad (13)$$

The travel time by low occupancy auto and high occupancy auto from location x to CBD $T_h^j(x)$ under HOVLP can be represented by $T_h^{la}(x)$ and $T_h^{ha}(x)$, respectively:

$$T_h^\tau(x) = \int_0^x t_h^\tau(w) dw, \forall x \in (0, L], \forall \tau = la, ha. \quad (14)$$

The disutility of traveling by bus from location x to CBD consists of the waiting time cost, the in-vehicles travel time cost, the in-vehicle passenger crowding discomfort cost and the bus fare. It can be represented as:

$$U_p^b(x) = \varepsilon_w w_p^b(x) + \varepsilon_t^b T_p^b(x) + G_p^b(x) + f_b, \forall p = m, e, h, \forall x \in (0, A], \quad (15)$$

where $T_p^b(x)$ is the in-vehicle travel time from location x to CBD, which can be determined with Eq. (6), (9) and (13). ε_t^b is the value of in-vehicle time of bus travelers, ε_w is the value of waiting time, and f_b is the bus fare.

The average waiting time of passengers at location x can be expressed by the volume-delay function (Li et al., 2009 and 2012):

$$w_p^b(x) = \frac{\gamma_1}{F_p} + \frac{\gamma_2}{F_p} \left(\frac{Q_b(x)}{O_b F_p} \right)^{\gamma_3}, \forall p = m, e, h, \forall x \in (0, A], \quad (16)$$

where F_p is the bus frequency for policy p (including MTP, EBLP and HOVLP) in the corridor, and γ_1 , γ_2 , and γ_3 are positive calibrated parameters that depend on the distribution of bus headway and passenger arrival times.

Passenger discomfort $G_p^b(x)$ is generally affected by the degree of crowding at bus stops and in carriages, which plays a significant role in mode choice because passengers may abandon the transit mode in favor of private auto travel when the discomfort becomes intolerable (Lam et al., 1999). The crowding discomfort cost per unit of in-vehicle travel time at location x is measured in terms of monetary units. It is assumed to be an increasing function of the passenger demand at location x as expressed by Eq. (17) (Huang et al., 2002):

$$g(x) = \iota_1 (Q_b(x))^2 + \iota_2 (Q_b(x)), \forall x \in (0, A], \quad (17)$$

where ι_1 and ι_2 are positive parameters.

The total in-vehicle crowding discomfort cost $G_p^b(x)$ of a passenger traveling from location x to CBD can be expressed as:

$$G_p^b(x) = \int_0^x g(w) t_p^b(w) dw, \forall p = m, e, h, \forall x \in (0, A], \quad (18)$$

where $t_p^b(w)$ is travel time per unit of distance for buses under various policies, as defined by Eqs. (5), (8) and (12).

As expressed in the delay equation (Dion et al., 2004; HCM 2010; Ge et al., 2013; Xie et al., 2023), the intersection delay per bus/auto at intersection i under different policies is:

$$d_{pj}^i = \frac{C_{signal}(1-\lambda)^2}{2(1-\min(1, \frac{\varpi_1}{\varpi_2})\lambda)} + 900t_I \left(\left(\frac{\varpi_1}{\varpi_2} - 1 \right) + \sqrt{\left(\frac{\varpi_1}{\varpi_2} - 1 \right)^2 + \left(8\kappa\varphi \frac{\varpi_1}{\varpi_2} \right) / (\varpi_2 t_I)} \right), \forall p =$$

$$m, e, h, \forall j = a, b, i \in [1, n_{inter}] \quad (19)$$

where d_{pj}^i is the intersection delay per bus/auto at intersection i under different policies, C is the lane capacity, C_{signal} is the cycle length, λ is the green signal ratio of the lane. t_I is the duration of analysis period, which represents the time interval over which traffic volume is measured. κ is an incremental delay factor accounting for pre-timed signal controller settings, and φ is the adjustment factor for upstream filtering.

The intersection delay per bus and auto is identical at intersection i due to the shared use of all lanes under MTP. The total volume at intersection i is computed by summing the cumulative volume of autos and buses between intersection i and $i + 1$, which is expressed by $\int_{l_i}^{l_{i+1}} \frac{q_a(x)}{O_a} dx + KF / (n_{inter} + 1)$. Under the EBLP and HOVLP, the delay functions differ due to variations in lane usage. In EBLP, buses and autos operate on separate lanes, whereas in HOVLP, high occupancy autos and buses use the dedicated lane, and low occupancy autos remain in the general-purpose lanes. Table 2 summarizes the intersection delay functions for both autos and buses under these distinct policies.

Table 2. Intersection delay functions under different policies

	Bus delay per vehicle (d_{pb}^i)	Auto delay per vehicle (d_{pa}^i)
MTP	$\varpi_1 = \int_{l_i}^{l_{i+1}} \frac{q_a(x)}{O_a} dx + KF / (n_{inter} + 1); \varpi_2 = n_{lane}C$	
EBLP	$\varpi_1 = KF / (n_{inter} + 1); \varpi_2 = C$	$\varpi_1 = \int_{l_i}^{l_{i+1}} \frac{q_a(x)}{O_a} dx; \varpi_2 = (n_{lane} - 1)C$
HOVLP	Bus / High occupancy auto	Low occupancy auto

$$\varpi_1 = (1 - \mu) \int_{l_i}^{l_{i+1}} \frac{q_a(x)}{o_a} dx + KF/(n_{inter} + 1); \varpi_2 = C \quad \varpi_1 = \mu \int_{l_i}^{l_{i+1}} \frac{q_a(x)}{o_a} dx; \varpi_2 = (n_{lane} - 1)C$$

The total intersection delay of bus travelers in the corridor is determined by summing the delay times across all intersections. To compute the total delay time of bus travelers at intersection i , it is necessary to first determine the total number of bus travelers at that intersection. This is represented by the cumulative travel demand of bus travelers from the location of intersection i to the city boundary. It can be expressed as follows:

$$D_p^b = \sum_{i=1}^{i=n_{inter}} \left(d_{pb}^i * \int_{l_i}^A Q_b(x) dx \right), \forall p = m, e, h, \quad (20)$$

where D_p^b denotes the intersection delay of buses under different policies.

The total cost of the bus users C_p^b under different policies can be obtained by accumulating the disutility from location x to CBD for bus passengers:

$$C_p^b = \int_0^A U_p^b(x) q_b(x) dx + \varepsilon_t^b D_p^b, \quad (21)$$

The bus operating cost C_p^o under different policies includes the fixed cost C_0^f and the variable cost C_0^v related to fleet size:

$$C_p^o = C_0^f + C_0^v (2T_p^b(A)F_p), \quad (22)$$

where $2T_p^b(A)F_p$ is the fleet size. The round-trip time $2T_p^b(A)$ can be determined with Eq. (6). C_0^f and C_0^v are the fixed and variable cost for bus operation, in dollars per hour.

The EBL/HOVL signal implementation cost C_p^s can be expressed as:

$$C_p^s = C_p^f + C_p^v A, \forall p = e, h, \quad (23)$$

where C_p^f and C_p^v are the fixed and variable parameters for EBL/HOVL signal implementation cost.

The travel disutility of the auto mode is the sum of travel time cost, delay cost and monetary cost (e.g., gas and parking cost):

$$U_p^a(x) = \varepsilon_t^a T_p^a(x) + \frac{(\delta_f^a + \delta_v^a x)}{o_a}, \forall p = m, e, \forall x \in (0, A], \quad (24)$$

where δ_f^a and δ_v^a are the fixed cost (e.g., parking cost) and variable cost (e.g., gas cost per unit of distance), ε_t^a is the value of in-vehicle time of auto users.

Because the auto under the HOVLP, the travel time and occupancy are different in the general lane and HPV lane, the travel disutility of the auto mode under HOVLP is expressed as:

$$U_h^a(x) = \varepsilon_t^a T_h^j(x) + (\delta_f^a + \delta_v^a x) / O_a^j, \forall j = la, ha, \forall x \in (0, A], \quad (25)$$

The total intersection delay for auto travelers under both MTP and EBLP can be obtained with Eq. (20). However, under HOVLP, the total delay differs because it is computed by summing the delays of low-occupancy and high-occupancy auto users separately. The total intersection delay of auto users D_p^a is:

$$D_p^a = \begin{cases} \sum_{i=1}^{i=n_{inter}} (d_{pa}^i * \int_{l_i}^A Q_a(x) dx), \forall p = m, e, \\ \sum_{i=1}^{i=n_{inter}} (d_{pla}^i * \int_{l_i}^A q_l Q_a(x) dx + d_{pha}^i * \int_{l_i}^A q_h Q_a(x) dx), \forall p = h, \end{cases} \quad (26)$$

where D_p^a is the total intersection delay of autos in the corridor.

The total travel cost of auto users C_p^a under different policies can be obtained by accumulating disutility from location x to CBD for all auto users:

$$C_p^a = \begin{cases} \int_0^A U_p^a(x) q_a(x) dx + \varepsilon_t^a D_p^a, \forall p = m, e, \\ \int_0^A U_h^{la}(x) \varepsilon_l q_a(x) dx + \int_0^A U_h^{ha}(x) \varepsilon_h q_a(x) dx + \varepsilon_t^a D_h^a, \forall p = h, \end{cases} \quad (27)$$

The total system cost of the corridor operating under different policies includes bus user travel cost C_p^b , bus operating cost C_p^o , travel cost of auto users C_p^a , and signal implementation cost of EBL and HOVL C_p^s . Therefore, the system cost minimization model for different policies can be formulated as Eq. (28):

$$\min C_{p\{F_p\}} = \begin{cases} C_p^b + C_p^o + C_p^a, \forall p = m, \\ C_p^b + C_p^o + C_p^a + C_p^s, \forall p = e, h. \end{cases} \quad (28)$$

$$s. t. F_p \geq \frac{\int_0^A q_b(x) dx}{O_b}, \quad (29)$$

The capacity constraint is defined in Eq. (29), ensuring that the transit service supply satisfies travel demand. The first-order optimality conditions for cost minimization model under different policies are outlined in Appendix A, and a solution algorithm is applied to solve this system cost minimization model. Given the demand density, the mode choice between bus and auto is determined once equilibrium

condition is achieved, as described in Appendix B. In this algorithm, R represents the ratio of auto demand to total demand in Eq. (2), serving as the mode choice at equilibrium condition. The solution algorithm for the cost minimization model is provided below.

Algorithm. Compute the system cost with corresponding optimal mode choice proportion and bus frequency

Require: travel demand density q , given mode choice proportion range \mathbf{R} , given bus frequency range \mathbf{F}

Ensure: the algorithm returns system cost of policy with mode choice proportions R^* and optimized bus frequency F^*

```

Define function  $C(q, \mathbf{R}, \mathbf{F})$ 
  Compute function  $R(q, \mathbf{R}, \mathbf{F})$ 
  Define function  $R(q, \mathbf{R}, \mathbf{F})$ 
    for  $R \in \mathbf{R}$  do
      Compute function  $F(q, R, \mathbf{F})$ 
      Define function  $F(q, R, \mathbf{F})$ 
        for  $F \in \mathbf{F}$  do
          Compute function  $C(q, R, F)$ 
          Until  $C(q, R, F)$  is minimal
        end for
      return  $F^* = \operatorname{argmin}C(q, R, F)$ 
      Compute function  $C(q, R, F^*)$ 
    until  $C^* = C(q, R, F^*)$  is minimal
  end for
  return  $R^* = \operatorname{argmin}C(q, R, F^*)$ 
return  $C^*$ 

```

3. Policy selection and schedules problem

The EBL and HOVL have been applied in some large U.S. cities. However, neither policy is suitable for application throughout an entire day due to the travel demand variation. Therefore, a dynamic model is developed in this section to optimize scheduling for different policies, including MTP, EBLP, and HOVLP. Using the previously established solution procedure, the optimal solutions of bus frequency denoted as F_p^* . Let $p1$ and $p2$ represent two different policies, respectively. Let F_{p1}^* and F_{p2}^* be the optimal solutions for the design variables of policies $p1$ and $p2$, respectively. They can be obtained by using the model and solution procedure proposed in the previous sections. Let $C_{p1}(F_{p1}^*(q_0^*))$ and $C_{p2}(F_{p2}^*(q_0^*))$ be the system cost levels associated with the policy $p1$ and $p2$, respectively. The policy selection and scheduling problem can then be formulated to maximize cost saving, as follows:

Definition 1 (Policy selection problem)

A threshold is determined by comparing each pair of policies; therefore, two thresholds exist with three policies. To simplify our equations and improve clarity, $p1$ and $p2$ are used to represent any two policies being compared. Here, $p1$ and $p2$ can be any two different policies from the set of three policies. Therefore, the system cost of one policy $p1$ dominates that of another policy $p2$ in the demand threshold if and only if the following conditions holds:

$$C_{p1}(F_{p1}^*(q_0^*)) \geq C_{p2}(F_{p2}^*(q_0^*)), \forall p = m, e, h, \quad (30)$$

where q_0^* is the demand threshold determining the policy entry and exit (i.e., start and stop). The optimized bus frequency F_p^* can be obtained from the first-order optimality conditions of the total cost function in Eq. (28). The first-order optimality conditions of the above cost function are given in Appendix A.

In this condition, the policy $p2$ is chosen because its total cost is lower; otherwise, the policy $p1$ is preferred.

Definition 2 (Switching timing for policy entry and exist)

Note that the costs of different policies are functions of the demand density. Naturally, this leads to the question of whether there is a demand density that induces an equal level of the system cost for different policies. It is further assumed that the demand density stochastically fluctuates over time as a non-stationary stochastic process. To adapt to this dynamic nature, the demand density is assumed to vary over time, adhering to the O-U process, which is a mathematical model used to describe the evolution of a continuous-time stochastic process (Guo et al., 2018). It can be expressed as:

$$dq_0 = v(\varpi - q_0)dt + \sigma q_0 dw, \quad (31)$$

where v is the mean reversion parameter, ϖ is long-term average demand density, σ is the volatility of the process, and dw is the increment of a standard Wiener process (Sødal et al., 2008). The time-varying demand density can be simulated as:

$$q_0(t) = q_0(0) \exp\left(-\left(v + \frac{\sigma^2}{2}\right)t + \sigma w\right) + \frac{\mu \bar{w}}{v + \frac{\sigma^2}{2}} \left(1 - \exp\left(-\left(v + \frac{\sigma^2}{2}\right)t\right)\right). \quad (32)$$

This effectively showcases the dynamic and time-sensitive characteristics of the demand density variability. After establishing the demand density thresholds between any two policies as outlined in Definition 1, demand density is simulated by the O-U process, as described in Eq. (32). Given the dynamic nature of demand density, which fluctuates over time, there are two critical timings within each scheduling period for the different policies: one where the demand density exceeds the threshold and another where it subsequently falls below the threshold. Given the policies $p1$ and $p2$ and their associated parameters, demand density becomes a trigger factor for starting policy $p2$ from $p1$ at t^1 and exiting policy $p2$ to $p1$ at t^0 , which is shown in Figure 3. The cumulative cost of different policies in each timing pairs can be obtained as:

$$W_p(\rho(t)) = W_p(t^o, t^\xi) = \int_{t^o}^{t^\xi} C_{p\{F_p^*\}}(q_0(t)) dt, \forall p = m, e, h, \quad (33)$$

where W_p is the cumulative cost in the schedules period for one policy, C_p represents the system cost associated with policy p , including MTP, EBLP, and HOVLP, which can be computed using Eq. (28)

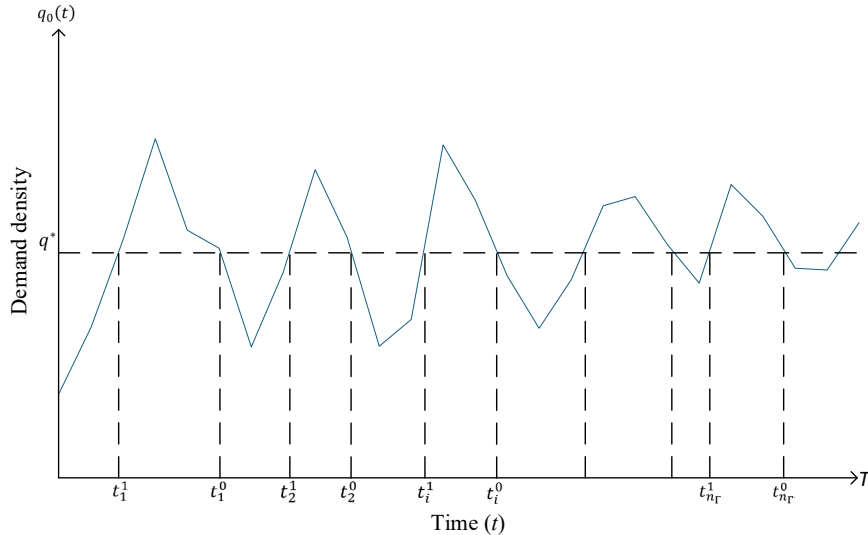


Figure 3. The timing of entry and exit

The operating policy is specified by function $\rho(t) \in \{0,1\}$, where 0 represents alternative policy

operating in timing pair (t^1, t^0) and 1 represents current policy operating in timing pair (t^0, t^1) . The operator decides whether to switch from $\rho(t - dt) = 0$ (or 1) in the previous time period dt to $\rho(t) = 1$ (or 0), where the operating policy impacts the system cost $W_p(\rho(t))$ in different timing pair. In the policy schedules problem, the objective is to find the feasible schedules period that maximizes total cost saving over the planning horizon T . Given the lane policies $p1$ and $p2$ and their associated parameters, the feasible lane policy schedule set $\Gamma = \{(t_1^1, t_1^0), (t_2^1, t_2^0), \dots, (t_{n_r}^1, t_{n_r}^0)\}$ should include all schedule periods in which the total cost of one policy dominates that of another policy if and only if the Definition 1 is satisfied. Therefore, the total cost saving can be formulated as:

$$Z = \max_{\{\rho(t)\}} \sum_0^{n_r} (W_{p1}(\rho(t)) - W_{p2}(\rho(t))). \quad (34)$$

4. Numerical analysis

The data in Table 3 are used in the following numerical analyses to demonstrate the model. These data are adopted from Li et al. (2009), Li et al. (2012) and Yao et al. (2018).

Table 3. Data baseline

Parameters	Definitions	Baseline values	Units
A	Distance between CBD and city boundary	30	mi.
C	Lane capacity	1500	veh/ hr.
C_0^f	Fixed cost of bus operation	300	\$
C_0^v	Variable cost of bus operation	20	\$/hr.
C_e^f	Fixed cost of EBL signal implementation	100	\$
C_e^v	Variable cost of EBL signal implementation	5	\$/hr.
C_h^f	Fixed cost of HOVL signal implementation	500	\$
C_h^v	Variable cost of HOVL signal implementation	10	\$/hr.
C_{signal}	Cycle length in the intersection	130	Sec.
K	Factor converting a bus into a number of autos with equivalent effect on traffic	3	-
f_b	Flat fare paid per bus trip	1	\$/per trip
n_{lane}	The number of lanes in the corridor	3	lane
O_{la}	Occupancy rate of low occupancy auto	1	pax/veh
O_{ha}	Occupancy rate of high occupancy auto	3	pax/veh
O_b	Bus capacity	70	pax/veh
t_0^a	Free-flow auto travel time per unit of distance	0.05	hr./mi.
t_0^b	Free-flow bus travel time per unit of distance	0.025	hr./mi.
t_l	Duration of the analysis setting method	1	hr.
α^a	Corrected parameter of BPR function	0.15	-

α^b	Corrected parameter of BPR function	0.15	-
β^a	Corrected parameter of BPR function	4	-
β^b	Corrected parameter of BPR function	4	-
ε_t^b	Value of in-vehicle time of bus travelers	15	\$
ε_t^a	Value of in-vehicle time of auto users	20	\$
δ_f^a	Fixed cost of auto usage	2	\$
δ_v^a	Variable cost of auto usage	0.3	\$/mi.
l_1	Positive parameters in discomfort function	0.000001	-
l_2	Positive parameters in discomfort function	0.005	-
μ	The fraction of low-occupancy autos over total autos	0.6	-
γ_1	A positively calibrated parameter that depends on the bus headway	0.5	-
γ_2	A positive parameter that is used to calibrate the distribution of passenger arrival times	0.05	-
γ_3	A positive parameter that is used to calibrate the distribution of passenger arrival times	2	-
λ	Green signal ratio of the lane	0.7	-
κ	Incremental delay factor accounting for pre-timed signal controller settings	0.5	-
φ	Adjustment factor for upstream filtering	1	-

4.1 Policy selection analysis

Figure 4 reflects the effect of demand density on total system costs of different policies including MTP, EBLP) and HOVLP. To show their variations more clearly, Figures 4a and 4b display the trend of demand density in 200-1200 pax/hr/mi and 1200-2200 pax/hr/mi, respectively. Under low demand density conditions, congestion effects in general-purpose lanes are minimal, due to traffic volume remaining well below road capacity. As a result, both MTP and EBLP produce very similar system costs when the demand density is below 600 pax/hr/mi. Additionally, when congestion effects are minimal, the impact of bus and auto shares on total costs is also limited, as travelers are not incentivized to switch modes when neither option has a significant travel cost advantage over the other. However, as demand density increases, greater congestion occurs in both general-purpose and special lanes. When the cost of a particular mode decreases, it becomes more attractive, promoting a significant shift in travelers' mode choices and resulting in a notable impact on overall system costs. Consequently, the system costs of different policies change significantly when demand density exceeds 600 pax/hr/mi.

From Figure 4a, it is evident that HOVLP emerges as the more favorable policy at relatively low demand densities (below 1072 pax/hr/mi) since it has the lowest system cost. At low density, the HOVL

remains largely uncongested, making it an efficient choice for low-demand periods where congestion effects are not a primary concern. As demand density increases (e.g., in Figure 4b), HOVLP becomes less favorable due to intensified traffic congestion, as evidenced by the sharp rise in auto travel cost shown in Figure 5b, which harms HOVL users. Since HOVL accommodates high-occupancy vehicles (HOVs) and buses, more passengers are affected compared with MTP and EBLP, thereby significantly increasing total system cost. Then, MTP becomes the more beneficial mode between 1072 pax/hr/mi and 2007 pax/hr/mi as HOVs enter the general-purpose lanes if the HOVL is more congested. Moreover, MTP proves beneficial by addressing the inefficiency of lane underutilization that can arise under dedicated-lane policies. Congestion is evenly distributed across all lanes under moderate demand, reducing the overall system cost by preventing bottlenecks specifically in HOVL or EBL. When demand density is high in Figure 4b, bus travelers tend to increase as potential travelers seek alternatives to avoid delays in general-purpose lanes. EBL enables buses to bypass congestion, reducing system costs by ensuring rapid public transit, which is essential in high-demand periods when road capacity is strained. Therefore, EBLP emerges as the most favorable policy in scenarios with extremely high demand density (above 2007 pax/hr/mi). Under MTP, where all types of vehicles share the lanes, congestion impacts all vehicles equally as demand grows. However, due to the higher occupancy rates of HOVs and buses, the system cost under HOVLP increases more rapidly than under MTP. As a result, the intersection points between HOVLP and EBLP occurs earlier than the intersection between MTP and EBLP. In summary, for policy selection, HOVLP is suitable when demand density is low, switching to MTP as demand increases, and ultimately shifting to EBLP during periods of very high demand.

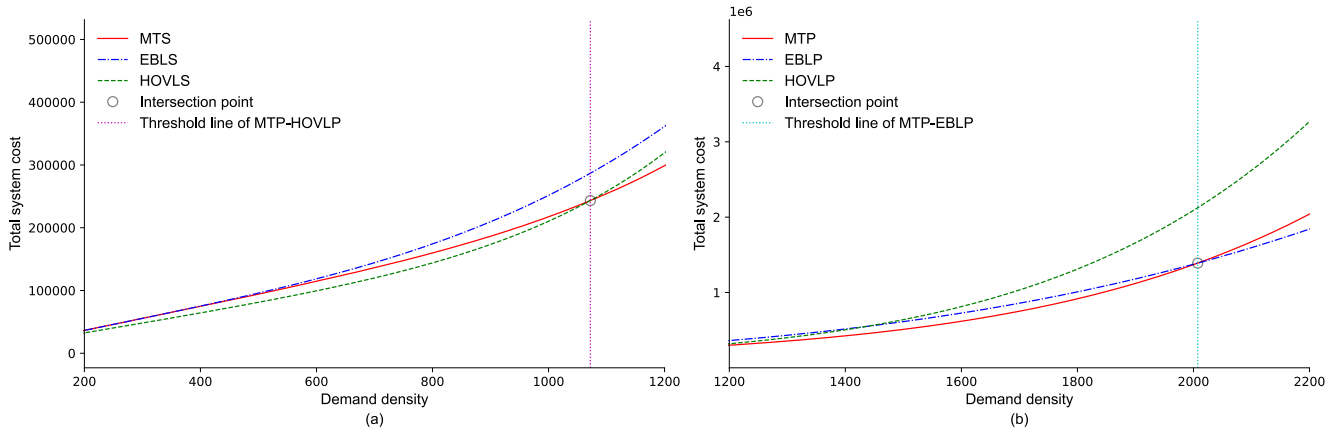


Figure 4. Total cost of different policies

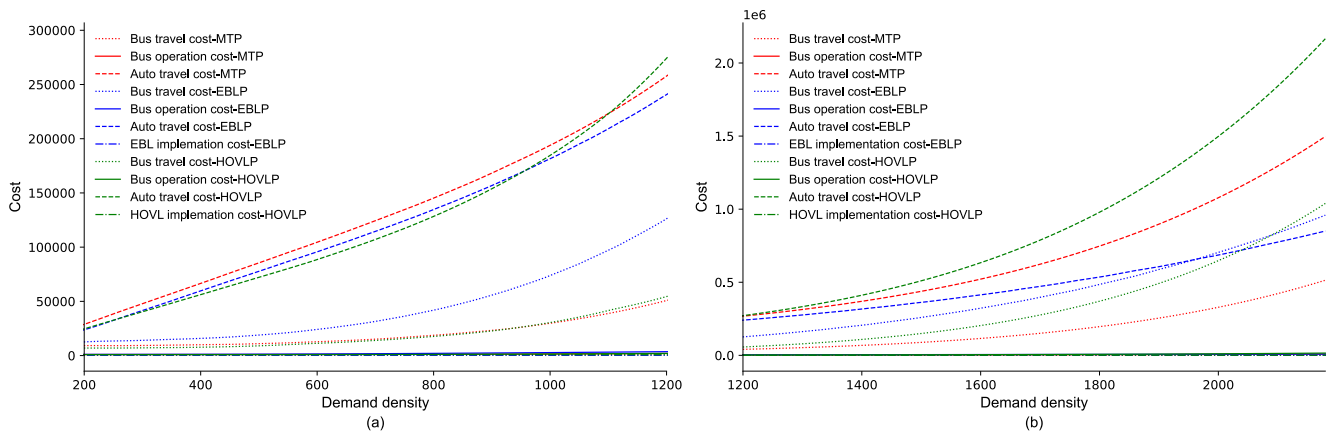


Figure 5. Breakdown of cost components

Figure 5 shows the trend of different cost components as demand density rises. For a more detailed view, two graphs (Figure 5a and b) are presented from low to high demand density range. The mode split between bus and auto obtained through the user equilibrium mode choice model is shown in Figure 6. Comparing Figures 4 and 5, indicates that the total system cost is primarily affected by the auto travel cost (dashed line) and bus travel cost (dotted line). According to Figures 5a and b, bus operating cost (solid line) and lane implementation cost (dash dot line) have the least impact on the total cost compared to travel cost of auto and bus, and it is difficult to observe their difference due to the magnitude difference from the other two costs. In Figure 5a, the auto travel cost dominates because most of travelers opting for auto travel, as shown in auto share in Figure 6. As demand density increases from Figures 5a to 5b, a larger

share of travelers shifts to bus travel, as indicated by the increased bus share under EBLP in Figure 6. This is because, as demand density increases, buses experience less congestion under EBLP, even as congestion intensifies in the general-purpose lanes. When demand density is high, bus travel cost rises due to more bus users. Meanwhile, auto travel cost under EBLP (blue dashed line) becomes lower than with other policies because the increase in bus demand decrease in the total cost of auto travelers. In Figure 6, the auto share increases when the demand density is relatively low (below 500 pax/hr/mi) for all policies. Since the increased demand at low demand densities does not cause congestion in the corridor, the auto share continues to grow. The highest bus share of EBLP indicating that the implantation of EBL attracts more bus users. As the demand density increases, congestion occurs in the general-purpose lanes, making the advantage of EBLP more apparent and thereby increasing the bus share. The general trends of mode split are similar for MTP and HOVLP, indicating that the travel cost of autos and buses have the same trend as the total cost.

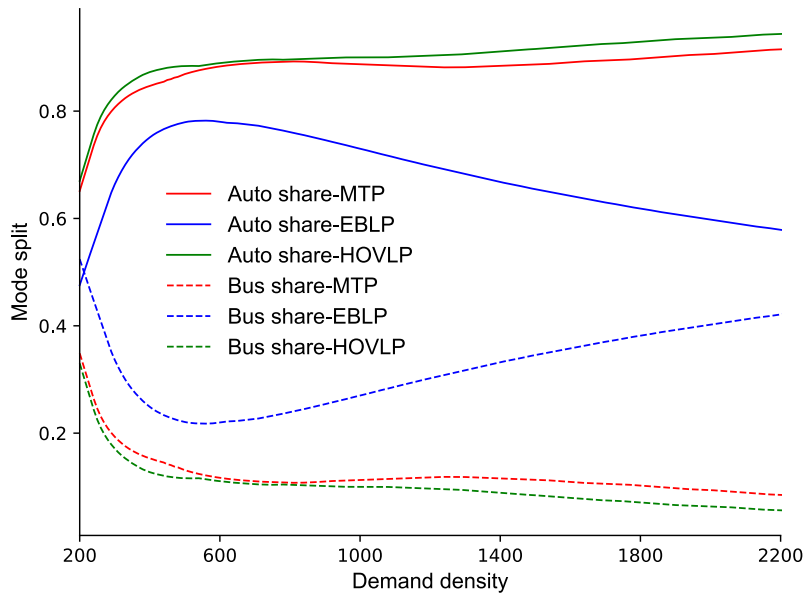


Figure 6. Mode split in the bi-modal transportation corridor

4.2 Effect of the road capacity on total cost

Figure 7 illustrates the variation in total system cost with demand density across different road capacities, ranging from 1200 to 1800 vehicles per hour. A larger C indicates that more road resources can be utilized

within the given time. As road capacity increases, the total system cost for all three policies decreases, as indicated by the progressively lower range of the Y-axis in Figures 7a1, 7b1, and 7c1. The cost difference between EBLP and MTP widens, and the intersection point changes from 1412 pax/hr./mi in Figure 7a2 to 2007 pax/hr./mi in Figure 7b2. This occurs because, in EBLP, an increase in road capacity delays the critical point at which the demand of auto travelers in general-purpose lanes exceeds the road capacity. As a result, EBLP becomes more advantageous, as the general-purpose lanes experience less congestion with increasing road capacity. For changes in the values of the Y-axis of the three lines, the decrease in total cost is most significant for EBLP as road capacity increases for all three policies. Additionally, Figures 7a1, 7b1 and 7c2, indicate that the cost difference between HOVLP and MTP widens before intersection point, and their intersection point changes from 863 pax/hr./mi. in Figure 7a1 to 1283 pax/hr./mi. in Figure 7c2. As road capacity increases, the point at which low-occupancy autos in general-purpose lanes under HOVLP reach the road capacity is delayed. Consequently, the benefits of HOVLP increase relative to MTP before their intersection point.

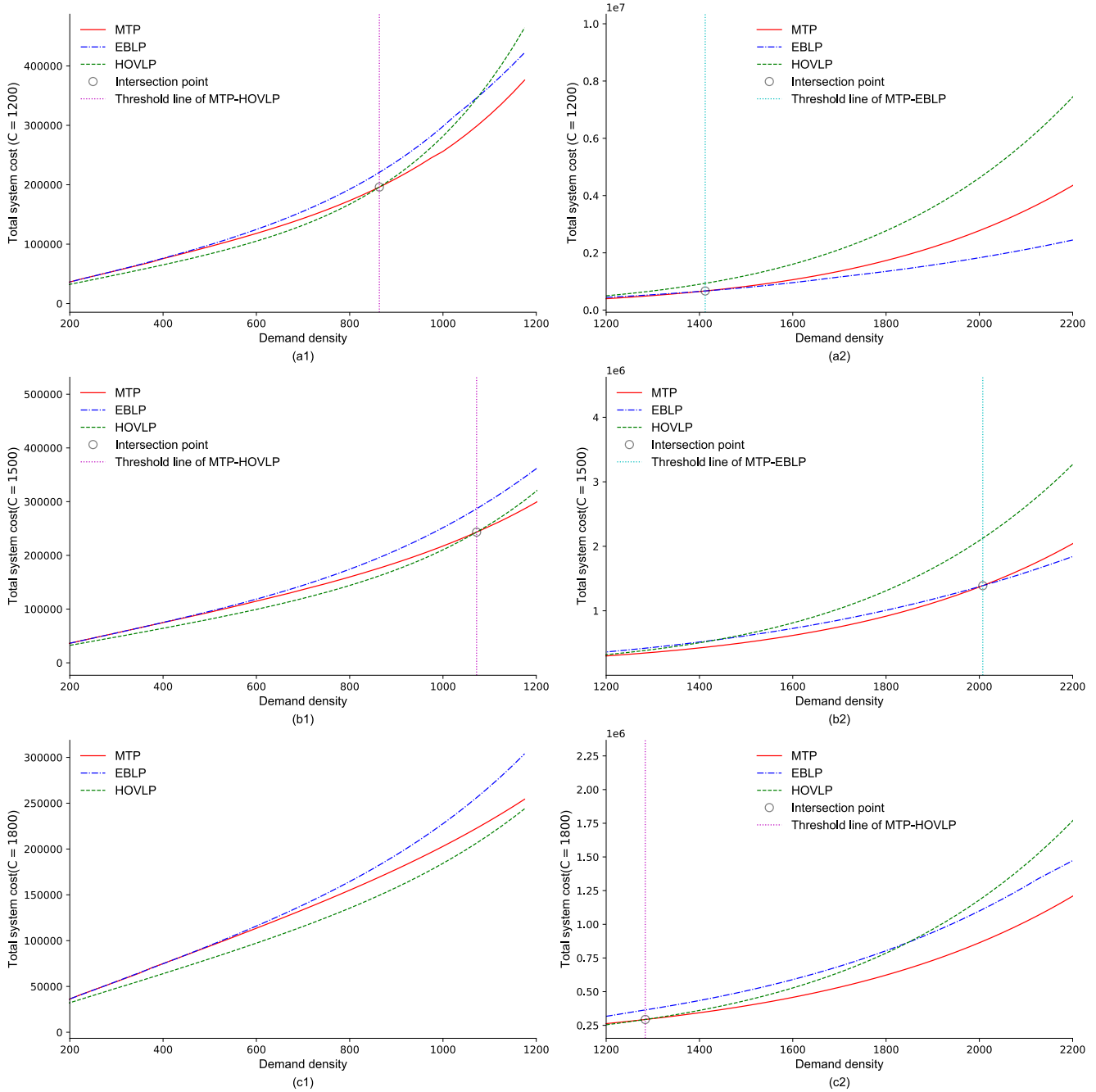


Figure 7. Effect of the road capacity on total cost

4.3 Optimized frequency

Figure 8 plots the optimized bus frequency for various policies. At first, the total cost initially decreases as bus frequency increases. This occurs because higher bus frequency reduces the waiting time for passengers, thereby lowering their travel cost and, consequently, the total cost. However, as bus frequency

continues to increase, the operation costs of the buses also rise. Thus, at a later stage, the total cost begins to increase as bus frequency increases. From Figure 8, the optimized bus frequencies are 16 for MTP, 20 for EBLP and 12 for HOVLP, respectively. This difference arises because the extent to which bus is affected by auto varies across different policies. Under the HOVLP, lanes are shared between bus and HOVs, which might lead to more congestion in the HOVL than under the MTP because the travel cost is higher in Figure 9. This additional congestion could make it less efficient to operate buses at a higher frequency, as the benefits of increased frequency would be offset by delays caused by interactions with other vehicles in the lane. Therefore, the bus frequency is lower under the HOVLP than under the MTP. Under EBLP, the waiting time and travel time of bus passengers are not influenced by auto because buses operate separately in EBL. The optimized bus frequency is highest compared with MTP and HOVLP. Therefore, bus operators need to offer higher frequencies when the reduction in travel cost exceeds the increase in operation cost. The predominant cost components that affect the optimized bus frequency are bus travel cost and bus operation cost, as shown in Figure 9, in which the left Y-axis represents the bus travel cost for different bus frequencies, while the right Y-axis indicates the bus operation cost.

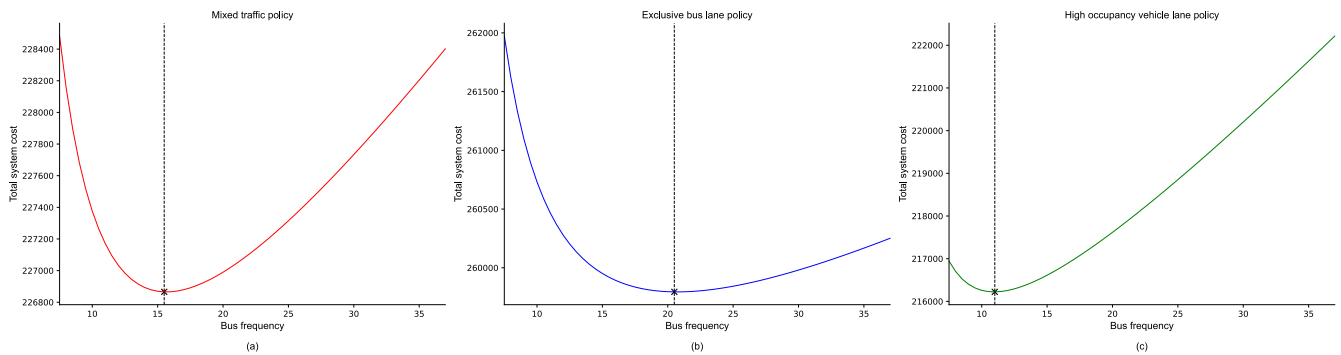


Figure 8. The optimized bus frequency under different policies

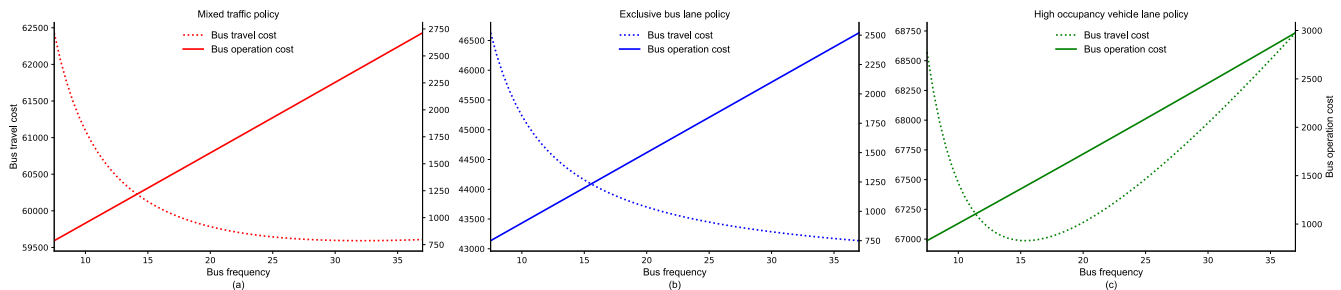


Figure 9. The optimized bus frequency under different policies

4.4 Policy schedules model analysis

In this section, three different types of schedules are analyzed using our proposed model, as outlined in Table 4. For Policy Schedules A and B, the schedules are optimized for each of the two policies (EBLP/HOVLP) with MTP based on the policy selection model. Two typical HOV and EBL corridors, I-5 and SR-99 in Seattle, have been selected as case studies for Schedules A and B and will be simulated using the OU process based on the parameter calibration from historical demand densities (Census Data 2020, Seattle). The schedules for various policies and their corresponding cost savings are evaluated based on demand density thresholds. Furthermore, combined policy schedules are introduced, incorporating transitions between the three policies. The model is validated using simulated demand density, and a schematic illustration of the three schedules is provided in Figure 10.

Table 4. Definition of conducted experiment and real-world cases

Proposed policy schedule	Policies switching	Experiment	Real-world case
Policy Schedule A: High occupancy lane schedules	Switching between HOVLP and MTP	--	Seattle I-5 corridor
Policy Schedule B: Exclusive bus lane schedule	Switching between EBLP and MTP	--	Seattle SR-99 corridor
Policy Schedule C: Combined policy schedule	Switching among HOVLP, MTP and EBLP	Simulated uncertainty demand density with O-U process	--

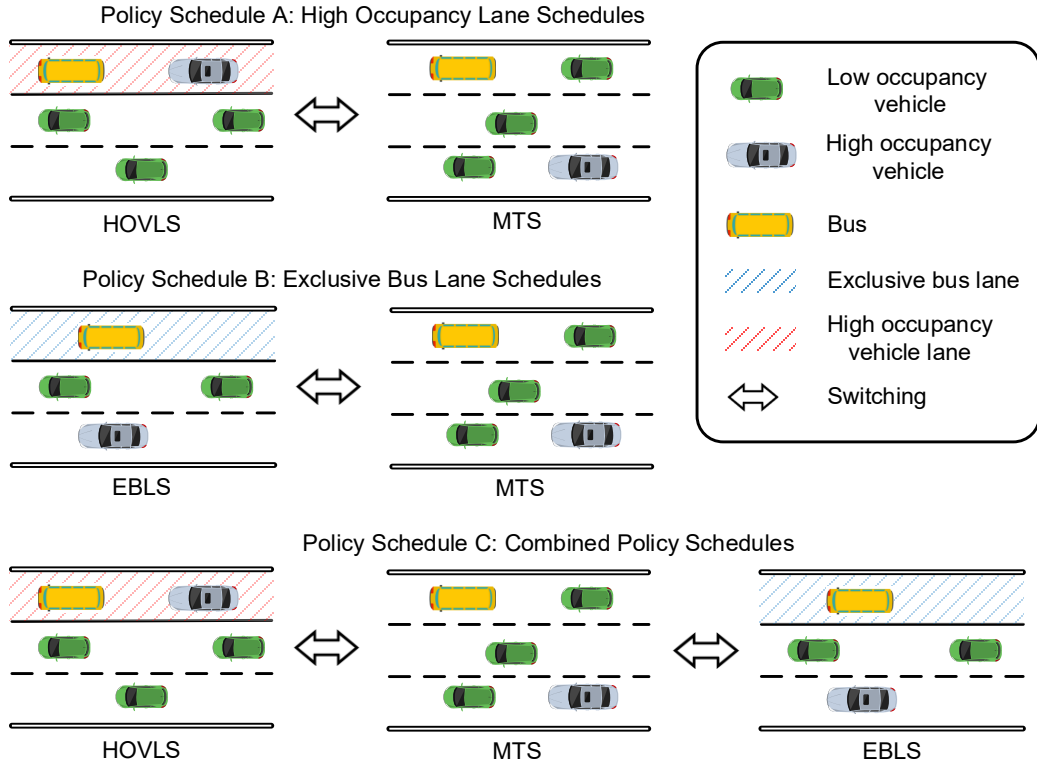


Figure 10. Schematic illustration of the three schedules

4.4.1 Experiment

As noted previously, the demand density in the Central Business District (CBD) over time is simulated using an O-U process (Sødal et al., 2008; Guo et al., 2017). Ten simulation trajectories or paths of the CBD’s demand density over time were simulated using Eq. (42) and shown in Figure 11. The total system cost of different policies can be determined after obtaining the simulated results according to O-U process. In the experiment, one trajectory will be chosen from the 10 trajectories shown in Figure 11. Based on the sample trajectory, the total cost of three policies at different time points are shown in Figure 12. The system costs of the three policies change as the demand density fluctuates. Therefore, the most favorable policy can be found at different time slots shown in Figure 12. Potential switching points (represented by the black circle) in the Figure 12 imply that the cost of one policy exceeds that of the other. If real-time switching is enabled by the lane control system, the three policies can be dynamically combined and switched based on variations in total cost. The vertical black lines in Figure 12 indicate the switching timing between different policies, signifying the transition from one policy to another more beneficial one.

The feasible switching timing under the infinite horizon setting are determined by Eqs. (44) and (45). Based on the results in Figure 12, the policy schedules can be obtained in Table 5. For example, we observe that the total system cost for each policy varies in response to changes in demand density. During different periods, the most beneficial policy is identified for different periods. Since HOVLP is optimal for periods with low demand density, only two time periods (7:31-8:01 and 14:32-15:45) are most favorable for implementing HOVLP. Therefore, HOVLP is scheduled for these periods in the timetable. In Table 5, The entry timing t^{entry} and exit timing t^{exit} , represent the timing when one policy switches to another.

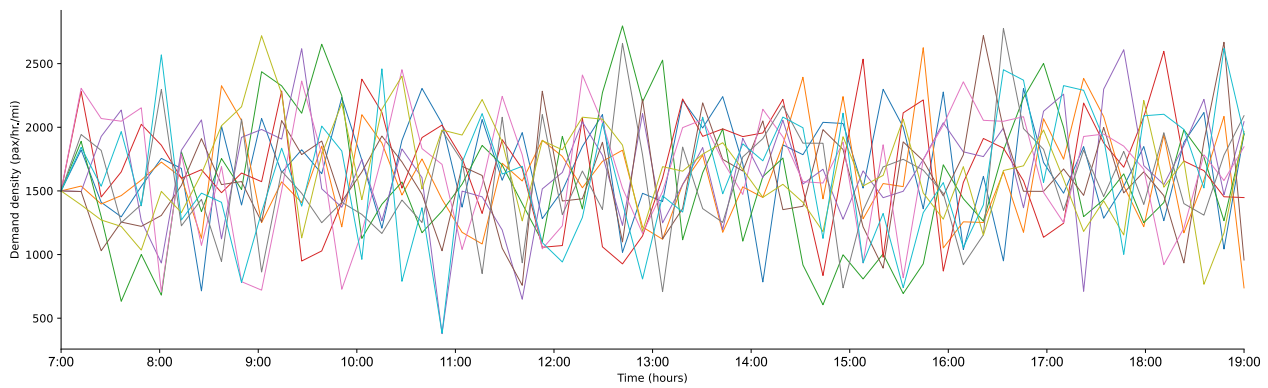


Figure 11. Simulated demand density by O-U process

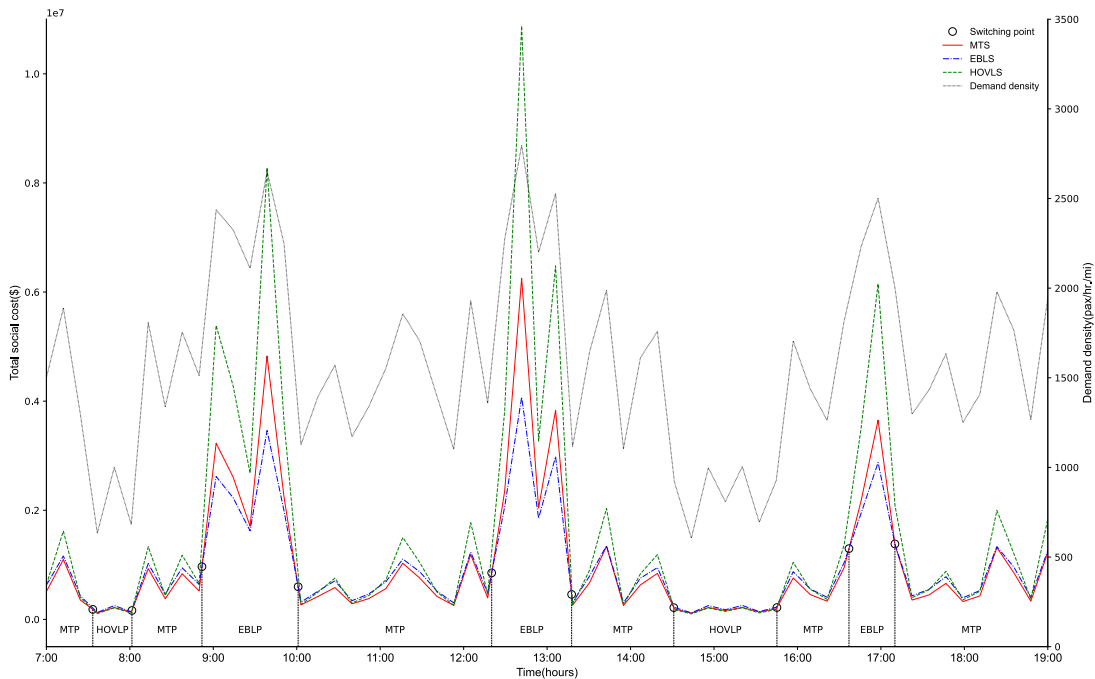


Figure 12. Optimized policy entry and exit timing overlaid onto one sample trajectory

Table 5. Optimized policy schedule under one simulated demand trajectory for the simulated trajectory shown in Figure 12.

Entry timing (t^{entry})	Exit timing (t^{exit})	Policy option	
7:00	7:31	MTP	
7:31	8:01		HOVLP
8:01	8:51	MTP	
8:51	10:00		EBLP
10:00	12:21	MTP	
12:21	13:17		EBLP
13:17	14:32	MTP	
14:32	15:45		HOVLP
15:45	16:37	MTP	
16:37	17:10		EBLP
17:10	19:00	MTP	

The cumulative costs of different policies over the 12-hours from 7 am to 7 pm in workdays are summarized in Table 6, where we find that the cumulative cost of policy schedule C (combined policy schedules) decreases compared to the single policy (MTP, EBLP and HOVLP only). Compared to single static policies (MTP, EBLP and HOVLP only), the proposed combined policy reduces the cost by 12.0%, 5.3% and 42.5%, respectively.

Table 6. Cumulative cost of different schedules in the simulated policies

	Traditional schedules			Proposed combined schedules	The cost saving compared with		
	MTP-only	EBLP-only	HOVLP-only		MTP-only	EBLP-only	HOVLP-only
Cumulative cost	11903526	11071533	18222020	10480218	12.0%	5.3 %	42.5%

4.4.2 Real-world case study

To implement the proposed policy schedules model for Schedule A and Schedule B, Interstate 5 (I-5) and State Route 99 (SR-99) in Seattle are used as two real-world case studies. As depicted in Figure 13, I-5 in the southern region of Seattle serves as a HOV lane corridor to Seattle’s CBD. The total length from Fife Heights to Downtown Seattle is 27.7 miles. According to census data (Census Data 2020, Seattle), the population in this area is approximately 54,280, with an average of 4 persons per household. Therefore,

there are about 13,570 households along this corridor. Assuming that 365 trips per household per year to the CBD and a peak hour factor of 0.1, the demand density in the CBD from I-5 can be estimated to be approximately 1,476 passengers per hour.

State Route 99 (SR-99), spanning from the northern outskirts of Seattle to the bustling CBD at its southern terminus, has been designated as an exclusive bus lane corridor. The total length of SR-99 in North Seattle is 26.9 miles. According to the census data and using the same parameters, the demand density in the CBD from SR-99 is about 1,245 passengers per hour. According to the Washington DOT (WSDOT), the speed limits for I-5 and SR-99 are 60 and 35 mph, respectively, so these two values are input as average speeds, while all other parameters are taken from Table 3.

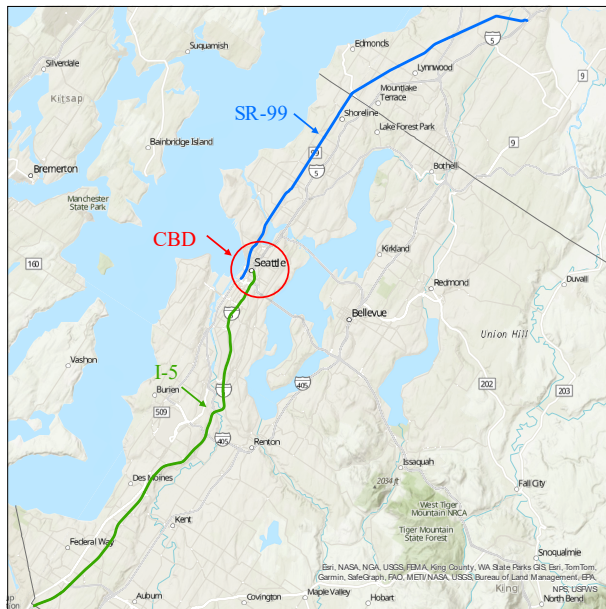


Figure 13. Two typical corridors in Seattle

Using the same computation process as in the experiments, costs associated with different policies under Schedule A and Schedule B are computed to determine the threshold for switching. The fluctuations in demand densities for these policies are simulated using the O-U process based on the actual demand density of two corridors. Utilizing our proposed policy schedules model, schedules for these two policies are derived and presented in Table 7. The entry timing and exit timing are still defined for the switching timing between two different policies and the more beneficial policy option over time detailed in Table 7.

In real-world corridors, the conditions for switching among the three policies in the experiment are infeasible. Unlike the experiments, our real-world case study utilizes existing HOVL and EBL corridors and applies our dynamic schedules according to the actual variation of demand. This demonstrates that our dynamic scheduling model can be effectively applied to existing EBL and HOVL corridors. Applying the Schedule A and B in the existing HOVL and EBL, the cost savings from implementing the proposed policy schedules are computed and shown in Table 8. It is evident that the proposed schedules result in the lowest costs across both cases. Schedule A reduces costs by 12.1% and 32.2% compared to the MTP and HOVL, respectively. Similarly, Schedule B reduces costs by 7.8% and 27.9% compared to the MTP and EBL, respectively.

Table 7. Policy schedules of real-world case studies

Schedule A applied in I-5			
Entry timing (t^{entry})	Exit timing (t^{exit})	Policy option	
7:00	8:18	MTP	
8:18	9:17		HOVLP
9:17	16:40	MTP	
16:40	18:02		HOVLP
18:02	19:00	MTP	
Schedule B applied in SR-99			
Entry timing (t^{entry})	Exit timing (t^{exit})	Policy option	
7:00	8:29	MTP	
8:29	12:09		EBLP
12:09	13:15	MTP	
13:15	19:00		EBLP

Table 8. Cumulative cost saving of different policies in two case studies.

Cumulative cost (\$/day)	Traditional schedules		Proposed schedule	The cost saving compared with traditional schedules	
	MTP	HOVLP	Schedule A	MTP	HOVLP
	11179546	14504266	9820634	12.1%	32.2%
	MTP	EBLP	Schedule B	MTP	EBLP
	10394331	13314507	9587753	7.8%	27.9%

5. Conclusion and future studies

A series of static models, namely total cost minimization models for the MTP, EBLP, and HOVLP, are

formulated for a commuter corridor. For a given demand input, the optimized bus frequency is thus found. The effect of the different parameters on different policies is revealed with case studies.

Major findings include the following:

- (1) Optimized bus frequency can be obtained for different policies in a transportation corridor. The tradeoff mainly occurs between the bus operation cost and the bus passengers' travel cost.
- (2) The total costs are dynamically influenced by the demand split between auto and bus usage. Initially, HOVLP is the most cost-efficient when demand density is below 1072 pax/hr/mi. MTP becomes advantageous in the range of 1072 pax/hr/mi to 2007 pax/hr/mi, while EBLP emerges as the preferable policy when demand density exceeds 2007 pax/hr/mi.
- (3) As road capacity increases, the anticipated decrease in auto travel costs under EBLP leads to a more significant decrease in total cost compared to MTP and HOVLP, while the widening cost difference between HOVLP and MTP highlights the increase in total system costs, primarily for auto travel cost.
- (4) In the experiment, the proposed combined policy schedules significantly reduce cumulative costs compared to individual policies (MTP, EBLP, and HOVLP), achieving reductions of 12.0%, 5.3% and 42.5% respectively.
- (5) By implementing the real-world cases of Policy Schedules A and Policy Schedules B, the cumulative costs decrease by approximately 32.2% and 27.9%, respectively, compared to the cumulative costs under existing HOVL and EBL policies.

This research has several limitations and may be improved in the following aspects.

- (1) Demand density may be formulated with different models such as Geometric Brownian motion and compared with O-U process.
- (2) The omission of access cost assumes a continuous space, but in reality, bus stops are discretely located; therefore, the access cost should be considered as a component of the user cost.

- (3) In actuality, the road capacity is uncertain due to disruptions such as flooding, and weather. The road capacity may be considered as the supply uncertainty in the future.
- (4) The many-to-one travel demand pattern does not consider the complexities of a more realistic many-to-many demand pattern with multiple origins and destinations along the corridor. Future research will incorporate a comprehensive model to better capture these variations and improve policy evaluations.

Appendix A

To obtain the optimized bus frequency, a sensitivity analysis-based approach and numerical search is used based on the first-order conditions of social cost minimization model. The details of a sensitivity analysis-based approach and a numerical search approach can be found in Ying and Yang (2005), and in Li et al. (2012). Taking MTP as an example, the system cost minimization problem can be expressed as:

$$\min C_M(F_m) = C_m^b + C_m^o + C_m^a = \int_0^A (\varepsilon_w w_m^b(x) + \varepsilon_t^b (\int_0^x t_m^b(w) dw) + \int_0^x g(w) t_m^b(w) dw + f_b) q_b(x) dx + C_o^f + C_o^v (2T_m^b(A)F) + \int_0^A (\varepsilon_t^a (\int_0^x t_m^a(w) dw) + \delta_f^a + \delta_v^a x) q_a(x) dx. \quad (A1)$$

The first-order condition of above equation with regard to bus frequency F_m can be obtained by setting $\frac{\partial C_M(F_m)}{\partial F_m} = 0$, as below.

$$\frac{\partial C_M(F_m)}{\partial F_m} = \int_0^A \left(\varepsilon_w \frac{\partial w_m^b(x, F_m)}{\partial F_m} + \varepsilon_t^b \frac{\partial \int_0^x t_m^b(w, F_m) dw}{\partial F_m} + \int_0^x g(w) \frac{\partial t_m^b(w, F_m)}{\partial F_m} dw \right) q_b(x) dx + 2C_o^v \left(\int_0^A \frac{\partial t_m^b(x, F_m)}{\partial F_m} dx F_m + \int_0^A t_m^b(x) dx \right) + \int_0^A \varepsilon_t^a \frac{\partial \int_0^x t_m^a(w, F_m) dw}{\partial F_m} q_a(x) dx = 0. \quad (A2)$$

The first-order condition of total system cost under EBLP and HOVLP, concerning bus frequency F_e and F_h can be derived similarly:

$$\frac{\partial C_E(F_e)}{\partial F_e} = \int_0^A \left(\varepsilon_w \frac{\partial w_e^b(x, F_e)}{\partial F_e} + \varepsilon_t^b \frac{dt_e^b(F_e)x}{dF_e} + \int_0^x g(w) \frac{dt_e^b(F_e)w}{dF_e} dw \right) q_b(x) dx + 2C_o^v \left(\frac{dt_e^b(F_e)A}{dF_e} F_e + t_e^b(F_e)A \right) = 0. \quad (A3)$$

$$\frac{\partial C_H(F_h)}{\partial F_h} = \int_0^A \left(\varepsilon_w \frac{\partial w_h^b(x, F_h)}{\partial F_h} + \varepsilon_t^b \frac{\partial \int_0^x t_m^b(w, F_h) dw}{\partial F_h} + \int_0^x g(w) \frac{\partial t_h^b(w, F_h)}{\partial F_h} dw \right) q_b(x) dx + 2C_o^v \left(\int_0^A \frac{\partial t_h^b(x, F_h)}{\partial F_h} dx F_h + \int_0^A t_h^b(x) dx \right) + \int_0^A \left(\varepsilon_t^a \frac{\partial \int_0^x t_h^a(w, F_h) dw}{\partial F_h} \right) ((1 - \mu) O_{ha} / (\mu O_{la} + (1 - \mu) O_{ha})) q_a(x) dx = 0 \quad (A4)$$

Appendix B

To allocate demand effectively in a bimodal corridor, it is crucial to reach a state where each traveler opts for the mode with the lower cost compared to the alternative mode. Once no traveler can find a more cost-effective travel mode, the congested corridor will achieve user equilibrium. According to Liu et al. (2009) and Li & Wang (2018), the user equilibrium conditions can be expressed as follows:

$$q_a(x) > 0 \Rightarrow U^a(x) \leq U^b(x), \quad (\text{B1})$$

$$q_b(x) > 0 \Rightarrow U^b(x) \leq U^a(x), \quad (\text{B2})$$

The above generalized travel disutility for the bus mode and auto mode, i.e., $U^a(x)$, and $U^b(x)$, are given by Eqs. (8) and (14), respectively. This definition states that at equilibrium, the individual generalized travel disutility by a mode at any location should be lower or equal to another mode if the mode is used by commuters at that location.

They are proven that with given the demand density $q(x)$, $x \in [0, A]$, the user equilibrium mode choice $\left(R^* = \frac{q_a^*(x)}{q(x)}, 1 - R^* = \frac{q_b^*(x)}{q(x)}\right)$ at location x is an optimal solution of the following minimization problem (Liu et al., 2009):

$$\min \int_0^A U^{a*}(x)q_a(x)dx + \int_0^A U^{b*}(x)q_b(x)dx, \quad (\text{B3})$$

$$\text{subject to } q_a(x) + q_b(x) = q(x), \forall x \in [0, A] \quad (\text{B4})$$

$$q_a(x) \geq 0, \forall x \in [0, A] \quad (\text{B5})$$

$$q_b(x) \geq 0, \forall x \in [0, A] \quad (\text{B6})$$

where $U^{a*}(x)$ and $U^{b*}(x)$ are optimal user disabilities in the user equilibrium conditions.

Using the functional analysis method for minimization, we get the optimality conditions of the problem (B3) as follows:

$$q_a^*(x)(U^{a*}(x) - \lambda(x)) = 0, \forall x \in [0, A] \quad (\text{B7})$$

$$U^{a*}(x) - \lambda(x) \geq 0, \forall x \in [0, A] \quad (\text{B8})$$

$$q_a^*(x) \geq 0, \forall x \in [0, A] \quad (\text{B9})$$

$$q_b^*(x)(U^{b*}(x) - \lambda(x)) = 0, \forall x \in [0, A] \quad (\text{B10})$$

$$U^{b*}(x) - \lambda(x) \geq 0, \forall x \in [0, A] \quad (\text{B11})$$

$$q_b^*(x) \geq 0, \forall x \in [0, A] \quad (\text{B12})$$

The above conditions show that $\lambda(x)$ is the equilibrium generalized travel cost of commuters leaving home at location x . Thus, all commuters at location x have the identical and minimal generalized travel cost at equilibrium regardless of the mode chosen there. Eqs. (B7)-(B9) and (B10)-(B12) state the choice of travelers of the auto mode and bus mode along the corridor, respectively. For a given bus frequency, the travel demand distribution along the corridor can be determined by the mode choice equilibrium formulation (B7) - (B12).

Appendix C

The fractions of low-occupancy auto travelers and high-occupancy auto travelers, relative to the total number of auto travelers, as well as the average occupancy per auto, can be determined based on the provided parameters. We utilize two equations to compute the fraction of low-occupancy auto travelers over the total number of auto travelers, denoted as q_l , and the fraction of high-occupancy auto travelers over the total number of auto travelers, denoted as q_h . The given parameters include the total number of auto travelers Q_a , the occupancy of low-occupancy autos O_{la} , the occupancy of high-occupancy autos O_{ha} , and the fraction of low-occupancy autos over total autos μ .

The total number of auto travelers is the sum of low-occupancy auto travelers Q_{la} and high-occupancy auto travelers Q_{ha} :

$$Q_{la} + Q_{ha} = Q_a. \quad (C1)$$

For both occupancy rates of high-occupancy auto and low-occupancy auto, dividing by their respective fractions of the total number of auto travelers yields the total number of auto travelers, which can be expressed as follows:

$$\frac{Q_{la}}{O_{la} \cdot \mu} = \frac{Q_{ha}}{O_{ha}(1-\mu)}. \quad (C2)$$

By joining the two equations we obtain the number of low-occupancy auto travelers Q_{la} and high-occupancy auto travelers Q_{ha} , as expressed below:

$$\begin{cases} Q_{la} + Q_{ha} = Q_a \\ \frac{Q_{la}}{O_{la} \cdot \mu} = \frac{Q_{ha}}{O_{ha}(1-\mu)} \end{cases} \quad (C3)$$

Then, Q_{la} and Q_{ha} can be solved as follow.

$$\begin{cases} Q_{la} = \frac{\mu Q_a O_{la}}{\mu O_{la} + (1-\mu) O_{ha}} \\ Q_{ha} = \frac{(1-\mu) Q_a O_{ha}}{\mu O_{la} + (1-\mu) O_{ha}} \end{cases} \quad (C4)$$

The q_l and q_h are determined as follows:

$$\begin{cases} q_l = \frac{Q_{la}}{Q_a} = \frac{\mu O_{la}}{\mu O_{la} + (1-\mu) O_{ha}} \\ q_h = \frac{Q_{ha}}{Q_a} = \frac{(1-\mu) O_{ha}}{\mu O_{la} + (1-\mu) O_{ha}} \end{cases} \quad (C5)$$

After determining q_l and q_h , the average occupancy of auto O_a can be obtained as follows:

$$O_a = \frac{Q_a}{\frac{q_l Q_a}{o_{la}} + \frac{q_h Q_a}{o_{ha}}} = \frac{o_{la} o_{ha}}{o_{ha} q_l + o_{la} q_h}. \quad (C6)$$

References

- Basso, L. J., Guevara, C. A., Gschwender, A., & Fuster, M. (2011). Congestion pricing, transit subsidies and dedicated bus lanes: Efficient and practical solutions to congestion. *Transport Policy*, 18(5), 676-684.
- Berling, P., & Martínez-de-Albéniz, V. (2011). Optimal inventory policies when purchase price and demand are stochastic. *Operations research*, 59(1), 109-124.
- Boriboonsomsin, K., & Barth, M. (2008). Impacts of freeway high-occupancy vehicle lane configuration on vehicle emissions. *Transportation Research Part D: Transport and Environment*, 13(2), 112-125.
- Boysen, N., Briskorn, D., Schwerdfeger, S., & Stephan, K. (2021). Optimizing autopool formation along high-occupancy vehicle lanes. *European Journal of Operational Research*, 293(3), 1097-1112.
- Brownstone, D., Ghosh, A., Golob, T. F., Kazimi, C., & Van Amelsfort, D. (2003). Drivers' willingness-to-pay to reduce travel time: evidence from the San Diego I-15 congestion pricing project. *Transportation Research Part A: Policy and Practice*, 37(4), 373-387.
- Census Data, Seattle. <https://data-seattlecitygis.opendata.arcgis.com/datasets/annual-population-and-housing-estimates-for-2020-census-blocks-in-seattle/explore?location=47.663259%2C-122.356499%2C14.80>
- Chiabaut, N., & Barcet, A. (2019). Demonstration and evaluation of an intermittent bus lane strategy. *Public Transport*, 11(3), 443-456.
- Chow, J. Y., & Regan, A. C. (2011). Network-based real option models. *Transportation Research Part B: Methodological*, 45(4), 682-695.
- Chow, J. Y., & Regan, A. C. (2011). Real option pricing of network design investments. *Transportation science*, 45(1), 50-63.
- Chow, J. Y., Regan, A. C., Ranaiefar, F., & Arkhipov, D. I. (2011). A network option portfolio management framework for adaptive transportation planning. *Transportation Research Part A: Policy and Practice*, 45(8), 765-778.
- Chu, C. P., Tsai, J. F., & Hu, S. R. (2012). Optimal starting location of an HOV lane for a linear monocentric urban area. *Transportation Research Part A: Policy and Practice*, 46(3), 457-466.
- Cohen, M. C., Jacquillat, A., Ratzon, A., & Sasson, R. (2022). The impact of high-occupancy vehicle lanes on autopooling. *Transportation research part A: policy and practice*, 165, 186-206.
- Coscia, P., Braca, P., Millefiori, L. M., Palmieri, F. A., & Willett, P. (2018). Multiple Ornstein–Uhlenbeck processes for maritime traffic graph representation. *IEEE Transactions on Aerospace and Electronic Systems*, 54(5), 2158-2170.
- Currie, G., & Lai, H. (2008). Intermittent and dynamic transit lanes: Melbourne, Australia, experience. *Transportation Research Record*, 2072(1), 49-56.

- Dahlgren, J. (1998). High occupancy vehicle lanes: Not always more effective than general purpose lanes. *Transportation Research Part A: Policy and Practice*, 32(2), 99-114.
- Dion, F., Rakha, H., & Kang, Y. S. (2004). Comparison of delay estimates at under-saturated and over-saturated pre-timed signalized intersections. *Transportation Research Part B: Methodological*, 38(2), 99-122.
- Fontes, T., Fernandes, P., Rodrigues, H., Bandeira, J. M., Pereira, S. R., Khattak, A. J., & Coelho, M. C. (2014). Are HOV/eco-lanes a sustainable option to reducing emissions in a medium-sized European city?. *Transportation Research Part A: Policy and Practice*, 63, 93-106.
- Ge, X. Y., Li, Z. C., Lam, W. H., & Choi, K. (2013). Energy-sustainable traffic signal timings for a congested road network with heterogeneous users. *IEEE Transactions on Intelligent Transportation Systems*, 15(3), 1016-1025.
- Goh, K. C. K., Currie, G., Sarvi, M., & Logan, D. (2014). Bus accident analysis of routes with/without bus priority. *Accident Analysis & Prevention*, 65, 18-27.
- Guo, Q. W., Chen, S., Schonfeld, P., & Li, Z. (2018). How time-inconsistent preferences affect investment timing for rail transit. *Transportation Research Part B: Methodological*, 118, 172-192.
- Guo, Q. W., Chow, J. Y., & Schonfeld, P. (2017). Stochastic dynamic switching in fixed and flexible transit services as market entry-exit real options. *Transportation research procedia*, 23, 380-399.
- Guo, Q., Chen, S., Sun, Y., & Schonfeld, P. (2023). Investment timing and length choice for a rail transit line under demand uncertainty. *Transportation Research Part B: Methodological*, 175, 102800.
- Guo, Q., Sun, Y., Schonfeld, P., & Li, Z. (2021). Time-dependent transit fare optimization with elastic and spatially distributed demand. *Transportation Research Part A: Policy and Practice*, 148, 353-378.
- HCM 2010: Highway Capacity Manual. (2010). Washington, D.C.: Transportation Research Board.
- Ho, H. W., Wong, S. C., Yang, H., & Loo, B. P. (2005). Cordon-based congestion pricing in a continuum traffic equilibrium system. *Transportation Research Part A: Policy and Practice*, 39(7-9), 813-834.
- Ho, Y. L. (2013). *Bi-objective optimization of exclusive bus lane allocation and scheduling problem in cities* (Doctoral dissertation, UTAR).
- Hossain, M., & McDonald, M. (1998). Modelling the impacts of reducing non-motorised traffic in urban corridors of developing cities. *Transportation Research Part A: Policy and Practice*, 32(4), 247-260.
- Huang, H. J. (2002). Pricing and logit-based mode choice models of a transit and highway system with elastic demand. *European Journal of Operational Research*, 140(3), 562-570.
- Huang, D., Xing, J., Liu, Z., & An, Q. (2021). A multi-stage stochastic optimization approach to the stop-skipping and bus lane reservation schemes. *Transportmetrica A: Transport Science*, 17(4), 1272-1304.
- Javid, R. J., Nejat, A., & Hayhoe, K. (2017). Quantifying the environmental impacts of increasing high

occupancy vehicle lanes in the United States. *Transportation research part D: transport and environment*, 56, 155-174.

- Khoo, H. L., Teoh, L. E., & Meng, Q. (2014). A bi-objective optimization approach for exclusive bus lane selection and scheduling design. *Engineering Optimization*, 46(7), 987-1007.
- Khoo, H. L., & Ong, G. P. (2015). Bi-objective optimization approach for exclusive bus lane scheduling design. *Journal of Computing in Civil Engineering*, 29(5), 04014056.
- Kim, D., Ko, J., Xu, X., Liu, H., Rodgers, M. O., & Guensler, R. (2019). Evaluating the environmental benefits of median bus lanes: Microscopic simulation approach. *Transportation Research Record*, 2673(4), 663-673.
- Kittelson and Associates, Incorporated. TRB's Transit Cooperative Research Program (TCRP) Report 100: Transit Capacity and Quality of Service Manual, 2nd ed. Transportation Research Board, Washington, D.C., 2003.
- Lam, W. H., Cheung, C. Y., & Lam, C. F. (1999). A study of crowding effects at the Hong Kong light rail transit stations. *Transportation Research Part A: Policy and Practice*, 33(5), 401-415.
- Levin, M. W., & Khani, A. (2018). Dynamic transit lanes for connected and autonomous vehicles. *Public Transport*, 10, 399-426.
- Levinson, H. S., Lennon, L., & Cheng, J. (1991). Downtown Space for Buses--The Manhattan Experience. *Transportation Research Record*, (1308).
- Li, T., Ma, J., & Hale, D. K. (2020). High-occupancy vehicle lanes on the right: an alternative design for congestion reduction at freeway merge, diverge, and weaving areas. *Transportation letters*, 12(4), 233-245.
- Li, Z. C., Guo, Q. W., Lam, W. H., & Wong, S. C. (2015). Transit technology investment and selection under urban population volatility: A real option perspective. *Transportation research part B: methodological*, 78, 318-340.
- Li, Z. C., Huang, H. J., & Yang, H. (2020). Fifty years of the bottleneck model: A bibliometric review and future research directions. *Transportation research part B: methodological*, 139, 311-342.
- Li, Z. C., Lam, W. H., & Wong, S. C. (2009). The optimal transit fare structure under different market regimes with uncertainty in the network. *Networks and Spatial Economics*, 9, 191-216.
- Li, Z. C., Lam, W. H., & Wong, S. C. (2012). Modeling intermodal equilibrium for bimodal transportation system design problems in a linear monocentric city. *Transportation Research Part B: Methodological*, 46(1), 30-49.
- Li, Z. C., & Wang, Y. D. (2018). Analysis of multimodal two-dimensional urban system equilibrium for cordon toll pricing and bus service design. *Transportation Research Part B: Methodological*, 111, 244-265.
- Li, Z. C., Yao, M. Z., Lam, W. H., Sumalee, A., & Choi, K. (2015). Modeling the effects of public bicycle

- schemes in a congested multi-modal road network. *International Journal of Sustainable Transportation*, 9(4), 282-297.
- Liu, T. L., Huang, H. J., Yang, H., & Zhang, X. (2009). Continuum modeling of park-and-ride services in a linear monocentric city with deterministic mode choice. *Transportation Research Part B: Methodological*, 43(6), 692-707.
- Lu, X., Wang, J., Yuen, C. W., & Zheng, S. (2023). Exclusive bus lane allocation considering multimodal traffic equity based on bi-level programming. *Applied Sciences*, 13(4), 2047.
- Lv, D., Wu, Q., Chen, B., & Jiang, Y. (2021). Research on Decision Evaluation Model of HOV Lane Setting. *Scientific Programming*, 2021, 1-15.
- Navarrete-Hernandez, P., & Zegras, P. C. (2023). Mind the perception gap: The impact of bus rapid transit infrastructure on travelers' perceptions of affective subjective well-being. *Transportation Research Part A: Policy and Practice*, 172, 103670.
- Othman, K., Shalaby, A., & Abdulhai, B. (2023). Dynamic bus lanes versus exclusive bus lanes: Comprehensive comparative analysis of urban corridor performance. *Transportation Research Record*, 2677(1), 341-355.
- Russo, A., Adler, M. W., & van Ommeren, J. N. (2022). Dedicated bus lanes, bus speed and traffic congestion in Rome. *Transportation Research Part A: Policy and Practice*, 160, 298-310.
- Sharifi, F., Meitiv, A., Shelton, J., Xu, X., Burriss, M., Vallamsundar, S., & Xu, Y. A. (2022). Regional traffic operation and vehicle emission impact assessment of lane management policies. *Research in transportation economics*, 91, 101067.
- Sødal, S., Koekebakker, S., & Aadland, R. (2008). Market switching in shipping—A real option model applied to the valuation of combination carriers. *Review of Financial Economics*, 17(3), 183-203.
- Stamos, I., Kitis, G., Basbas, S., & Tzevelekis, I. (2012). Evaluation of a high occupancy vehicle lane in central business district Thessaloniki. *Procedia-Social and Behavioral Sciences*, 48, 1088-1096.
- Sun, Y., Guo, Q., Schonfeld, P., & Li, Z. (2017). Evolution of public transit modes in a commuter corridor. *Transportation Research Part C: Emerging Technologies*, 75, 84-102.
- Szarata, M., Olszewski, P., & Bichajło, L. (2021). Simulation study of dynamic bus lane concept. *Sustainability*, 13(3), 1302.
- Teer, A., Cuthbertson, T., & Carson, G. (1994). Public transport initiatives in Surrey. *Traffic engineering & control*, 35(2).
- The Transit Cooperative Research Program (TCRP). (2013). *Report 165: Transit capacity and quality of service manual* (3rd ed.). Washington, D.C: Transportation Research Board of the National Academies.
- Viegas, J., & Lu, B. (2004). The intermittent bus lane signals setting within an area. *Transportation Research Part C: Emerging Technologies*, 12(6), 453-469.

- Viegas, J., Lu, B., Vieira, J., & Roque, R. (2006). Demonstration of the intermittent bus lane in Lisbon. *IFAC Proceedings Volumes*, 39(12), 239-244.
- Wang, J. P., Huang, H. J., & Ban, X. J. (2019). Optimal capacity allocation for high occupancy vehicle (HOV) lane in morning commute. *Physica A: statistical Mechanics and its Applications*, 524, 354-361.
- Wang, J. Y., Yang, H., & Lindsey, R. (2004). Locating and pricing park-and-ride facilities in a linear monocentric city with deterministic mode choice. *Transportation Research Part B: Methodological*, 38(8), 709-731.
- Wang, X., & Li, Q. (2014). Utilization of the spare capacity of exclusive bus lanes based on a dynamic allocation strategy. *Urban Transport XX*, 138, 173-178.
- Wang, A., Wang, J., Zhang, R., & Cao, S. J. (2024). Mitigating urban heat and air pollution considering green and transportation infrastructure. *Transportation Research Part A: Policy and Practice*, 184, 104079.
- Wiseman, Y. (2019). High occupancy vehicle lanes are an expected failure. *International Journal of Control and Automation*, 12(11), 21-32.
- WSDOT - Roadway Data Speed Limits | WSDOT - Roadway Data Speed Limits | Washington State Geospatial Open Data Portal
- Wu, D., Deng, W., Song, Y., Wang, J., & Kong, D. (2017). Evaluating operational effects of bus lane with intermittent priority under connected vehicle environments. *Discrete Dynamics in Nature and Society*, 2017.
- Xie, X., Dong, L., Feng, L., Zhang, L., & Li, H. (2023). Modelling Method on Dynamic Optimal Setting and Associated Control for Intermittent Bus Lane. *Journal of Advanced Transportation*, 2023(1), 9487812.
- Xu, S. X., Liu, T. L., Huang, H. J., & Liu, R. (2018). Mode choice and railway subsidy in a congested monocentric city with endogenous population distribution. *Transportation Research Part A: Policy and Practice*, 116, 413-433.
- Yang, H. (1998). When should carpool lanes be introduced in a multi-lane highway? *Journal of advanced transportation*, 32(2), 242-252.
- Yang, H., & Huang, H. J. (1999). Carpooling and congestion pricing in a multilane highway with high-occupancy-vehicle lanes. *Transportation Research Part A: Policy and Practice*, 33(2), 139-155.
- Yao, J., Cheng, Z., Shi, F., An, S., & Wang, J. (2018). Evaluation of exclusive bus lanes in a tri-modal road network incorporating carpooling behavior. *Transport Policy*, 68, 130-141.
- Yao, J., Shi, F., An, S., & Wang, J. (2015). Evaluation of exclusive bus lanes in a bi-modal degradable road network. *Transportation Research Part C: Emerging Technologies*, 60, 36-51.
- Yao, J., Shi, F., Zhou, Z., & Qin, J. (2012). Combinatorial optimization of exclusive bus lanes and bus

frequencies in multi-modal transportation network. *Journal of Transportation Engineering*, 138(12), 1422-1429.

- Ying, J. Q., & Yang, H. (2005). Sensitivity analysis of stochastic user equilibrium flows in a bi-modal network with application to optimal pricing. *Transportation research Part B: methodological*, 39(9), 769-795.
- Yu, D. P., Li, Z. C., Liu, B., & Nguyen-Phuoc, D. Q. (2023). Transit-oriented development and floor area ratio regulation in a transportation corridor: Formulation and a case study. *Transportation Research Part A: Policy and Practice*, 176, 103814.
- Zhang, J., Wang, D. Z., & Meng, M. (2018). Which service is better on a linear travel corridor: Park & ride or on-demand public bus? *Transportation Research Part A: Policy and Practice*, 118, 803-818.
- Zhang, X., Yang, H., Huang, H. J., & Zhang, H. M. (2005). Integrated scheduling of daily work activities and morning-evening commutes with bottleneck congestion. *Transportation Research Part A: Policy and Practice*, 39(1), 41-60.
- Zhao, J., & Zhou, X. (2018). Improving the operational efficiency of buses with dynamic use of exclusive bus lane at isolated intersections. *IEEE Transactions on Intelligent Transportation Systems*, 20(2), 642-653.
- Zhong, L., Zhang, K., Nie, Y. M., & Xu, J. (2020). Dynamic autopool in morning commute: Role of high-occupancy-vehicle (HOV) and high-occupancy-toll (HOT) lanes. *Transportation Research Part B: Methodological*, 135, 98-119.
- Zhou, G., Mao, L., Hu, P., Sun, F., & Bao, X. (2020). Research on HOV lane priority dynamic control under connected vehicle environment. *Journal of Advanced Transportation*, 2020, 1-12.